UNIVERSITY OF TWENTE.

Faculty of Electrical Engineering,
Mathematics & Computer Science

Minimizing the start-up energy of a 3-stage inverter crystal oscillator

Christian H. Top

B.Sc. Thesis
June 2018

Supervisors:
dr. ir. R. A. R. van der Zee
J. B. Lechevallier MSc.
dr. ir. A. B. J. Kokkeler

Integrated Circuit Design Group
Faculty of Electrical Engineering,
Mathematics and Computer Science
University of Twente
P.O. Box 217
7500 AE Enschede
The Netherlands

Abstract

Crystal oscillators are commonly used components in electronic circuits to generate a certain frequency. In order to start-up a crystal oscillator, a negative resistance is needed. In classical methods often a single inverter is used to start-up the oscillator. However, the negative resistance of this single inverter stage implementation is limited, which increases the start-up time and therefore the start-up energy. In order to remove this limit on the negative resistance, a three-stage inverter implementation with capacitive loads can be used. This circuit has several design freedoms, which all have a certain effect on the total start-up energy. In this research an analysis is presented in which the influence of the different design parameters on the start-up energy is investigated. From this analysis it followed that for increasing values of the transconductance of each inverter stage, the start-up energy increases rapidly, so the increase in gain does not compensate the increase in energy. Furthermore it was found that the negative resistance can theoretically become infinitely big for certain combinations of parameter values. However, it is also demonstrated that when the negative resistance increases, the effect of parameter variations also increases. This increasing sensitivity to parameter variations can cause the negative resistance to become positive, which means that the crystal oscillator will not operate anymore. Therefore a safety margin can be defined when determining the value of the negative resistance. Furthermore the start-up energy that can be achieved with the single stage inverter implementation is determined and compared with the minimum start-up energy that is achieved with the three stage inverter implementation. From this comparison it followed that the three stage inverter has a start-up energy that is several orders of magnitude lower than the start-up energy of the single stage inverter. The calculations performed during the analysis are tested with different simulations. With these simulations it is verified that the energy consumption indeed decreases for decreasing values of the transconductance. Furthermore it followed from the simulations that due to the small transconductance the final amplitude of the oscillation is limited. However, in order to increase the amplitude with a certain factor, the start-up energy increases with a factor that is considerably higher. Therefore the amplitude of the oscillation should be kept as low as possible.

Contents

Chapter 1

Introduction

Crystal oscillators are components that are widely used in electronic systems. A crystal oscillator generates a certain frequency with a high precision, which makes them useful in circuits where timing is important. One of the application areas in which crystal oscillators play an important role is in wireless sensor networks. These networks often contain a lot of sensor nodes, which all collect data. This data needs to be sent to a central base station, so a radio is needed in order to send this information. From an energy point of view, it is beneficial to collect the data over a certain period of time, and only transmit the data at the end of each period (also known as duty-cycling). This is especially beneficial if the data rate is low. However, because the radio contains a crystal oscillator, the crystal needs to start-up every time the radio is going to be used. In order to start-up a crystal oscillator, a considerable amount of energy is needed. Because sensor nodes often operate on batteries, it is important to minimize this start-up energy in order to increase the battery life.

In order to start-up a crystal oscillator, a negative resistance is needed. This negative resistance is generated by the oscillator circuit. The negative resistance should be as big as possible in order to allow a fast start-up. A commonly used circuit for a crystal oscillator contains a single inverter in order to drive the crystal. However, the maximum negative resistance that can be generated by this single inverter is limited. This will be further explained in chapter 2. In order to remove this limit on the negative resistance, three inverter stages with capacitive loads can be used, as is demonstrated in [1]. However, this circuit has several design freedoms, which all have a certain effect on the total start-up energy of the crystal oscillator. In this research the optimum design parameters of this kind of circuit will be explored.

In this report, first some basic knowledge on crystal oscillators will be presented in chapter 2. Next, chapter 3 gives a general analysis on the three-stage inverter circuit with capacitive loads. In the chapter that follows the optimum design parameters are investigated using numerical calculations, and in chapter 5 these results will be verified using circuit simulations. This finally leads to the conclusions and recommendations, which are given in chapter 6.

Chapter 2

Oscillator basics

Before the optimum parameters of the three-stage inverter crystal oscillator will be investigated, first some general knowledge on crystal oscillators will be given in this chapter.

2.1 Model of the resonator

A crystal resonator can be modeled by an electrical equivalent circuit, as shown in figure 2.1. This electrical equivalent circuit consists of an inductor (L_M), a capacitor (C_M) and a resistor (R_M) in series. The inductor and the capacitor represent the motional components of the resonator, and the resistor R_M represents the loss of the resonator. Besides this series branch of L_M, C_M and R_M, there is also an additional parallel capacitance (C_S). This capacitance is introduced due to the leads and electrodes of the resonator. A crystal can generally oscillate at every odd harmonic of the fundamental frequency [2], in which each mode of oscillation has its own series branch characterized by an L_M, C_M and R_M value. However, the undesired modes are often very weakly coupled, or the different modes are not exact multiples of each other. Therefore the additional series branches can be neglected when an oscillation occurs at a certain single mode [3].

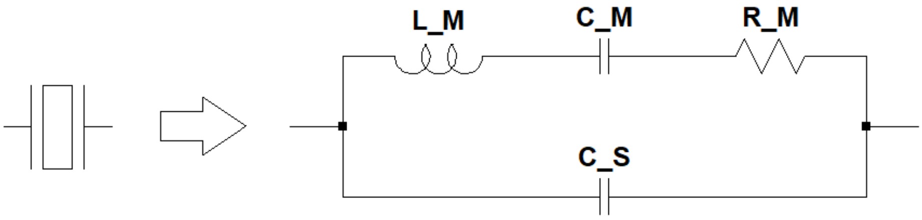

Figure 2.1: Electrical equivalent circuit of the resonator

2.2 The oscillator circuit

In order to drive the resonator, an electrical circuit is needed. Such a circuit generally consists of an amplifier and a feedback network. For the oscillator circuit, the crystal acts as the feedback network. For the amplifier, an inverter is often used. A schematic picture of the oscillator circuit is given in figure 2.2.

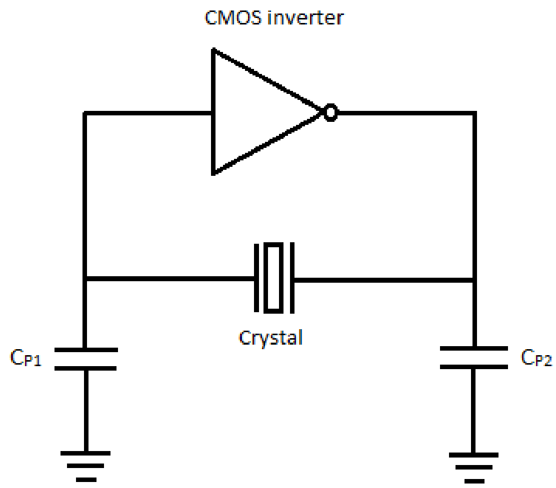

Figure 2.2: General Pierce oscillator circuit with parallel capacitances and single inverter

The crystal can both operate in series resonance mode as well as in parallel resonance mode. In order to allow an oscillation, two capacitors are connected at each of the two nodes of the crystal, as can be seen in figure 2.2. These two capacitances form a capacitor voltage divider that determines the degree of feedback [4]. The total parallel capacitance C_P is given by:

$$C_P = \frac{C_{P1}C_{P2}}{C_{P1} + C_{P2}} \tag{2.1}$$

C_P should be equal to the recommended load C_L of the crystal, which is usually specified in the manufacturers datasheet. In order to achieve the largest load capacitance for the least amount of total capacitance, equal values should be chosen for both of the parallel capacitances. When inserting this condition in equation 2.1, and using the fact that $C_P = C_L$, the values for the capacitances C_{P1} and C_{P2} can be found as follows:

$$C_L = \frac{C_{P1}C_{P2}}{C_{P1} + C_{P2}} \tag{2.2}$$

Because $C_{P1} = C_{P2}$, let $C = C_{P1} = C_{P2}$ for convenience. Equation 2.2 then becomes:

$$C_L = \frac{C^2}{2C} = \frac{C}{2} \tag{2.3}$$

$$C = 2C_L \tag{2.4}$$

So therefore it can be concluded that the capacitances C_{P1} and C_{P2} should have a value of $2C_L$.

2.3 Single-stage g_m implementation

As discussed in the previous section, a commonly used circuit for making a crystal oscillator is by using a single inverter. In this way a negative resistance R_N is generated, which is equal to the real part of the impedance Z_{C-1} (see figure 2.3). This negative resistance is needed to compensate for the loss in the resonator. In order to allow a fast start-up, this negative resistance should be as big as possible, as can be seen in equation 2.5 [5]:

$$\tau = \frac{2L_M}{R_M + R_N} \tag{2.5}$$

In this equation τ is the time constant, which is proportional to the total start-up time of the oscillator. An expression for the start-up time will be derived in section 3.4. From equation 2.5 it becomes clear that in order to reduce the time constant (which results in a shorter start-up time), the negative resistance R_N should be as big as possible. In order to optimize the negative resistance, an expression for R_N needs to be found. As already mentioned, the negative resistance consists of the real part of the impedance Z_{C-1}, which is defined in figure 2.3. From this figure it becomes clear that the negative resistance depends on the stray capacitance of the resonator C_S and the impedance of the amplifier circuit Z_{amp-1} (which also includes the load capacitances). In figure 2.3 the name of the different impedances is followed by the number 1. This indicates that the circuit with the single inverter is considered. Later on in this report, when the three-stage inverter system will be analysed, the name of the different impedances is followed by the number 3.

In appendix A.1 an expression for the negative resistance is derived as a function of the stray capacitance and the real and imaginary part of Z_{amp-1}. The resulting expression can be found in equation 2.6:

$$R_N = \frac{Re(Z_{amp})}{(\omega_0 C_S Re(Z_{amp}))^2 + (1 - \omega_0 C_S Im(Z_{amp}))^2} \tag{2.6}$$

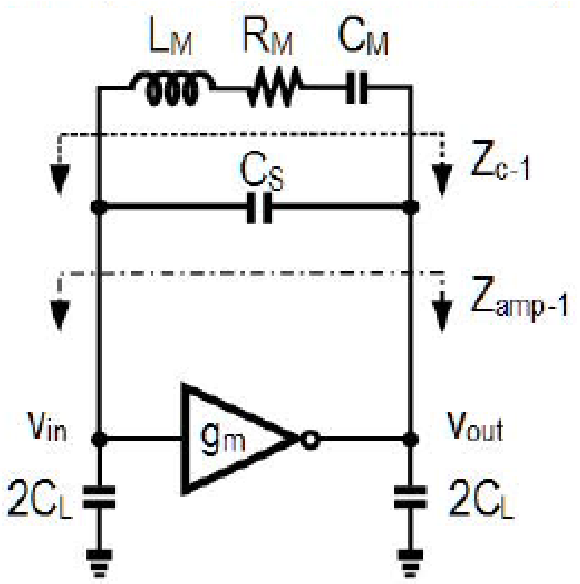

Figure 2.3: Oscillator circuit with a single inverter [1]

From equation 2.6 it follows that in order to determine the value of R_N, the impedance Z_{amp-1} should be determined. This impedance is given by equation 2.7 [1]:

$$Z_{amp-1} = -\frac{g_m}{4\omega_0^2 C_L^2} - j\frac{1}{j\omega_0 C_L} \tag{2.7}$$

When the expression for Z_{amp-1} is substituted in equation 2.6, the following expression for R_{N1} is obtained [1]:

$$R_{N1} = -\frac{4 g_m C_L^2}{(g_m C_S)^2 + 16 C_L^2 \omega_0^2 (C_L + C_S)^2} \tag{2.8}$$

From equation 2.7 it becomes clear that the imaginary part of Z_{amp-1} is negative (i.e. capacitive). This limits the minimum (i.e. the optimum) value of R_N due to the capacitance C_S, according to equation 2.6. The minimum value of R_{N1} can be found by differentiating equation 2.8. When this is done, the following result is obtained [1]:

$$R_{N1,min} = -\frac{C_L}{2\omega_0 C_S (C_L + C_S)} \tag{2.9}$$

This minimum value of R_{N1} appears for a g_m which is given by [1]:

$$g_m = 4\omega_0 C_L (1 + \frac{C_L}{C_S}) \tag{2.10}$$

In section 4.5 it will be investigated whether this minimum value of R_{N1} will also result in the minimum start-up energy.

In order to remove the limit on the minimum value for R_N, the imaginary part of Z_{amp} should be made positive (inductive), as can be seen in equation 2.6. How this can be achieved is explained in the next chapter.

Chapter 3

Three-stage g_m implementation

As discussed in the previous chapter, in order to remove the limit for the maximum value of R_N, the imaginary part of Z_{amp} should be made positive (i.e. inductive). This can be achieved by using 3 inverters with capacitive loads after each inverter stage (see figure 3.1). In this way, when a sinusoidal voltage is generated at the input, a current will start to flow through the capacitor after the first inverter. This current generates a voltage, but for a capacitor, this voltage occurs a small time instant later than the current. Therefore the current at the output of the second inverter will also be delayed. This delayed current will result in a voltage over the second capacitor, but again a small delay is added. The voltage at the output of the second stage will finally cause a current flow at the output of the third stage, but as became clear, this current occurs a small time instant later than the voltage that was generated at the input. In other words, the current is lagging behind the voltage, and therefore the impedance of the three inverters with the capacitive loads acts as an inductor.

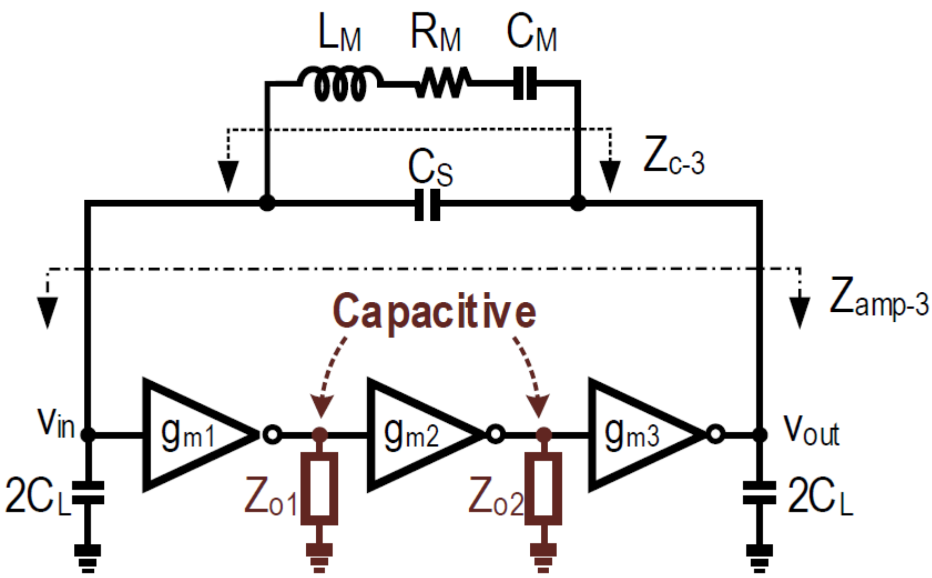

Figure 3.1: Oscillator circuit with three inverters and capacitive loads [1]

The implementation of the three inverter stages is given in figure 3.2. It is chosen to use resistive loads instead of current source loads in order to allow a small supply voltage V_{DD} [1].

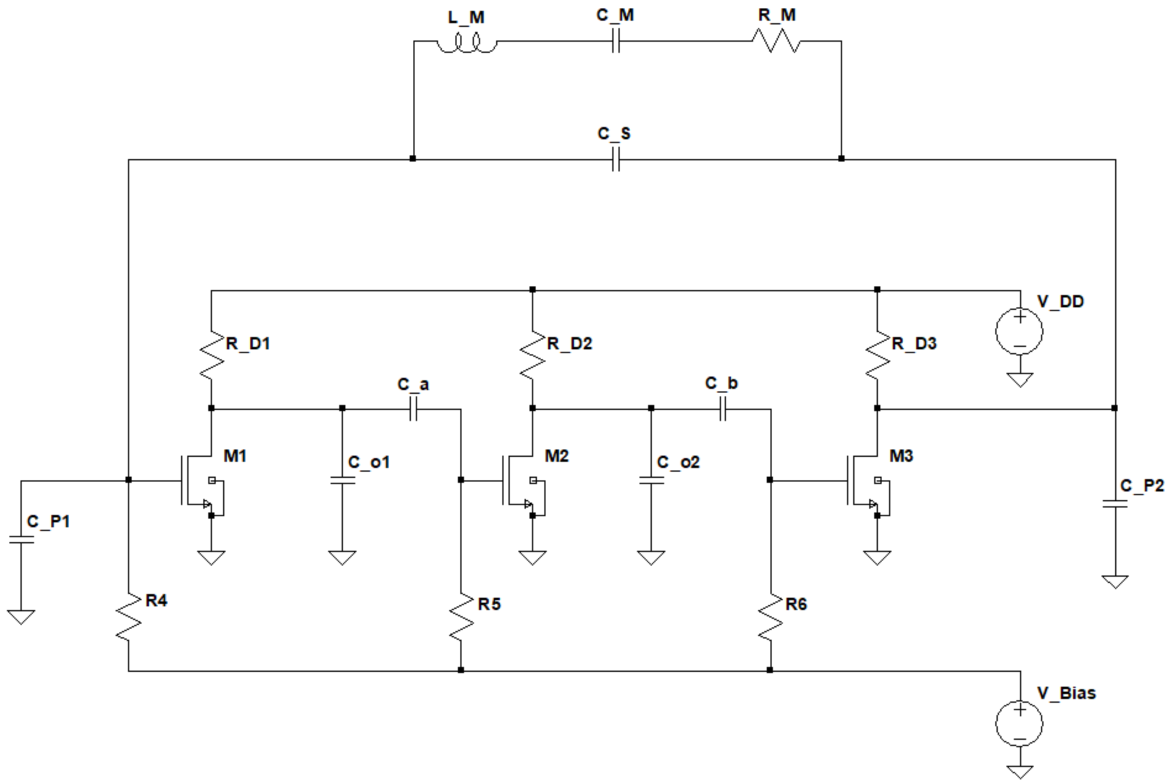

Figure 3.2: Implementation of the three inverter stages

In order to determine the impedance Z_{amp-3} (see figure 3.1) of this circuit, a small signal equivalent circuit (SSEC) is made, which can be found in figure 3.3. In this circuit the resistances R_{inv1} and R_{inv2} represent the total resistance of the first and the second inverter, respectively. When only small signals are considered the drain resistor R_D is connected in parallel to the output resistor r_o of the MOSFET. This means that the resistance R_{inv} of each inverter stage is defined as:

$$R_{inv} = R_D // r_o = \frac{R_D r_o}{R_D + r_o} \tag{3.1}$$

When the output resistance r_o of the MOSFET is much smaller than the drain resistance R_D, the resistance R_{inv} will be approximately equal to the value of r_o. Furthermore the total small signal resistance of the third inverter stage R_{inv3} is not incorporated in the SSEC. This is done because for typical oscillators the parallel (load) capacitances typically are in the pico-Farad range. This results in an impedance at the output of the third inverter stage that will presumably be much smaller than the impedance of R_{inv3}. Therefore the impedance R_{inv3} can most likely be neglected.

A final remark that can be made is that a MOSFET contains several parasitic capacitances, such as the gate-drain capacitance and the gate-source capacitance. These capacitances typically have a value of several femto-Farads. Therefore these capacitances can be neglected as long as the values of the load capacitances are chosen sufficiently higher.

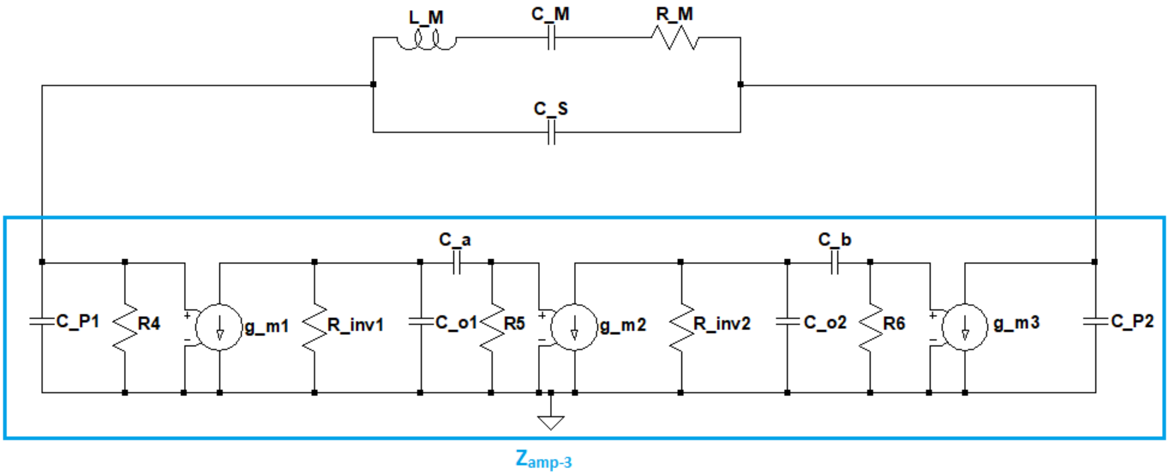

Figure 3.3: Small signal equivalent circuit of the crystal oscillator with the three g_m stages

Following these assumptions, the impedance Z_{amp-3} of the amplifier, when looking from the resonator (see figure 3.1), is given by equation 3.2.

$$\begin{aligned} Z_{amp-3} = &-\frac{g_{m1}r_{o1}g_{m2}r_{o2}g_{m3}(1-\omega_0^2 r_{o1}C_{o1}r_{o2}C_{o2})}{4\omega_0^2 C_L^2(1+(\omega_0 r_{o1}C_{o1})^2)(1+(\omega_0 r_{o2}C_{o2})^2)}+ \\ &j\frac{1}{\omega_0 C_L}(\frac{g_{m1}r_{o1}g_{m2}r_{o2}g_{m3}(r_{o1}C_{o1}+r_{o2}C_{o2})}{4C_L(1+(\omega_0 r_{o1}C_{o1})^2)(1+(\omega_0 r_{o2}C_{o2})^2)}-1) \end{aligned} \tag{3.2}$$

The derivation of this equation can be found in appendix A.2. In this equation for Z_{amp-3} it is assumed that the output resistance of the MOSFETs is much smaller than the drain resistor value R_D. When this equation will be used, it will be checked if this is indeed the case. Furthermore it is assumed that the values of the coupling capacitors C_a and C_b are chosen in such a way that they act as short circuits at the signal frequency. Therefore the coupling capacitors are also not taken into account in equation 3.2.

From equation 3.2 it becomes clear that $Im(Z_{amp-3})$ is now indeed positive (inductive) as long as the first term of $Im(Z_{amp-3})$ between brackets is bigger than one.

3.1 Energy consumption

As already became clear from chapter 2, a big R_N decreases the start-up time and therefore reduces the start-up energy. However, a maximum value for R_N does not necessarily result in the smallest energy consumption. For example, increasing the value of g_m may result in a bigger value of R_N, but it will also require more current, which increases the start-up energy. The total start-up energy can be calculated by using the following equation:

$$E_{total} = P \cdot t \tag{3.3}$$

$$E_{total} = U \cdot I \cdot t \tag{3.4}$$

In which t is the total start-up time. In the following subsections a short analysis will be given of the influences of the different parameters on the total start-up energy.

3.1.1 Transconductance (g_m)

In order to allow a fast start-up, the gain of the inverters should be as high as possible. The gain of a single inverter stage is given by the following equation:

$$A_V = g_m \cdot (R_D // r_o) \tag{3.5}$$

From this equation it follows that increasing the transconductance g_m with a factor x will also increase the gain with a factor x. When the gain becomes higher, the amplitude will grow faster, which reduces the start-up time. However, a higher g_m also requires a higher current, which will increase the start-up energy. Therefore a trade-off needs to be found.

Another option to increase the gain is by increasing the value of the drain resistor R_D, as becomes clear from equation 3.5.

3.1.2 Capacitive loads

As already became clear, Z_{amp-3} should be inductive in order to optimize the value of R_N. This means that the imaginary part of Z_{amp-3} should be positive. However, $Im(Z_{amp-3})$ should not be increased too much, because then the value of R_N will decrease again due to the fact that the second term of the denominator of equation 2.6 is squared. From equation 2.6 it follows that for the optimum value of R_N, the second term of the denominator of R_N should be zero. This poses the following condition on the imaginary part of Z_{amp-3}:

$$(1 - \omega_0 C_S Im(Z_{amp-3}))^2 = 0 \tag{3.6}$$

$$1 - \omega_0 C_S Im(Z_{amp-3}) = 0 \tag{3.7}$$

$$\omega_0 C_S Im(Z_{amp-3}) = 1 \tag{3.8}$$

$$Im(Z_{amp-3}) = \frac{1}{\omega_0 C_S} \tag{3.9}$$

Making Z_{amp-3} more inductive (in order to meet the condition mentioned in equation 4.1) means that the phase shift should be bigger, which means that the circuit should be made slower. This can be done by increasing the values of the capacitors C_{o1} and C_{o2}. In this way the RC product increases, which results in a bigger time constant and therefore the speed of the system will decrease. However, bigger capacitor values will also require more current in order to generate the gain, which will increase the energy consumption.

3.2 Design parameters

In order to find the optimum design parameters of the oscillator circuit, the parameters of the crystal should be known. The crystal is specified by its resistance R_M, its capacitance C_M, its inductance L_M and its stray capacitance C_S. The inductance of the resonator can be calculated using the value of the motional capacitance C_M and the operating frequency. When considering the parallel resosance frequency, the frequency can be calculated using equation 3.10 [6]:

$$\omega_p = \frac{1}{\sqrt{\frac{L_M C_M C_S}{(C_M + C_S)}}} \tag{3.10}$$

In order to calculate the value of the inductance, equation 3.10 can be rewritten to:

$$L_M = \frac{C_M + C_S}{\omega_p^2 C_M C_S} \tag{3.11}$$

Table 3.1 shows the parameters that are given. The parameters that are going to be optimized are shown in table 3.2.

Besides the parameters given in table 3.2, there are also some circuit parameters which do not directly influence the start-up energy of the crystal oscillator. These

Table 3.1: Given parameters of the oscillator

given parameter	parameter name
Motional inductance	L_M
Motional capacitance	C_M
Motional resistance	R_M
Stray capacitance	C_S
Load capacitance	C_L
Supply voltage	V_{DD}

Table 3.2: Parameters which have to be optimized

variable parameter	parameter name
Capacitive loads	C_{o1}, C_{o2}
Drain resistors	R_{D1}, R_{D2}, R_{D3}
Transconductances	g_{m1}, g_{m2}, g_{m3}

parameters are for example the coupling capacitances, the bias resistances and the bias voltage. Despite the fact that these components do not directly influence the start-up energy of the crystal oscillator, they play an important role in order to allow a proper operation of the system.

The coupling capacitors should be chosen in such a way that the $-3dB$ cut-off frequency is sufficiently lower than the operating frequency of the crystal. The required value of the coupling capacitor can be calculated using the following equation:

$$C = \frac{1}{2\pi f_{-3dB} R_{eq}} \tag{3.12}$$

In this equation R_{eq} is the input impedance of the inverter stage. The value of the coupling capacitor should be chosen sufficiently larger than the calculated capacitance C.

Furthermore, the bias resistors should be chosen considerably larger than the drain resistors, such that the signal is not attenuated. Finally, the bias voltage can be derived when the optimum value for g_m is found.

3.3 Supply voltage

In the previous section it was mentioned that the supply voltage V_{DD} is fixed, which is generally the case. Normally the supply voltage determines the final amplitude of the oscillation. However, it can be beneficial to choose a value of V_{DD} that is slightly higher than the desired final amplitude of the oscillation. This is because at the boundaries of the saturation region the gain is smaller than somewhere in the middle of the saturation region. When the amplitude of the supply voltage is chosen a bit higher, this effect of the decreased gain can be reduced. This means that the final amplitude can be reached in a shorter time which will reduce the start-up energy. However, increasing V_{DD} will also increase the start-up energy, according to equation 3.4. Therefore a trade-off needs to be found. When the desired amplitude is reached, the three-stage g_m circuit can be switched off and the single stage g_m circuit can be turned on in order to sustain the oscillation.

3.4 Start-up time

In order to determine the total start-up energy, the start-up time of the crystal oscillator should be known, according to equation 3.4. A commonly used definition for the start-up time of a crystal oscillator is the time it takes for the amplitude of the voltage across the resonator to reach the value of the supply voltage. This time can be defined as [5]:

$$t_{s,tot} = \tau ln(\frac{V_{DD}}{v(0)}) \tag{3.13}$$

In this equation $t_{s,tot}$ is the total start-up time, τ is the time constant, V_{DD} is the supply voltage and $v(0)$ is the initial value of the amplitude of the voltage across the resonator. Equation 3.13 can be rewritten to [5]:

$$t_{s,tot} = \tau ln(\frac{V_{DD}}{i(0)}\sqrt{\frac{C_T}{L_M}\frac{C_M + C_T}{C_M}}) \tag{3.14}$$

In this equation, $i(0)$ is the initial current flowing through the resonator, and C_T is the total capacitance seen from the resonator:

$$C_T = C_S + \frac{C_{P1}C_{P2}}{C_{P1} + C_{P2}} \tag{3.15}$$

In equation 3.14 it is assumed that the system is already connected to the power supply, and that the MOSFETS are already in saturation. However, when the amplitude of the voltage becomes higher than $V_{DD}/2$, usually nonlinear effects occur such that the amplitude does not grow exponentially anymore [5]. Therefore in this research the start-up time will be defined as the time that it takes for the amplitude of the voltage across the resonator to reach half the supply voltage. This time is given by [5]:

$$t_{s,half} = t_{s,tot} - \tau \cdot ln(2) \tag{3.16}$$

In order to determine the time constant τ, the following equation can be used [5]:

$$\tau = \frac{2L_M}{R_M + Re(Z_C)} \tag{3.17}$$

From equation 3.14 it became clear that in order to compute the total start-up time, the initial current through the resonator needs to be determined. This will be done in the next section.

3.4.1 Determining the initial current $i(0)$

In order to determine the current through the resonator at time $t = 0$, first of all the impedance of the resonator needs to be known. Using the Laplace notation, this impedance is given by:

$$Z_M = sL_M + R_M + \frac{1}{sC_M} \tag{3.18}$$

To start-up the oscillator, a voltage V is applied to the resonator. When this voltage is a step function, the initial current I through the resonator can be written as [5]:

$$I(s) = \frac{V(s)}{L_M s^2 + R_M s + \frac{1}{C_M}} \tag{3.19}$$

In order to calculate the initial current $i(0)$, the inverse Laplace transform has to be applied to equation 3.19. It is assumed that in order to start-up the crystal oscillator, a voltage is applied at time $t = 0$ to the resonator, which grows exponentially till it has reached the value of the supply voltage V_{DD}. In this way the following expression is obtained for the initial current $i(0)$ [5]:

$$i(0) = \frac{V_{DD}}{L_M t_0} \cdot \frac{1}{\sqrt{\frac{1}{L_M C_M} - (\frac{R_M}{2L_M})^2}} \cdot \frac{1}{\sqrt{\frac{1}{t_0^2} - \frac{R_M}{L_M t_0} + \frac{1}{L_M C_M}}} \tag{3.20}$$

This is approximately equal to [5]:

$$i(0) \approx \frac{V_{DD} C_M}{\sqrt{L_M C_M + t_0^2}} \tag{3.21}$$

When $t_0 = 0$, equation 3.21 becomes:

$$i(0) \approx \frac{V_{DD} C_M}{\sqrt{L_M C_M}} \tag{3.22}$$

This expression for $i(0)$ can be substituted in equation 3.14. When this is done the start-up time can be calculated for specified values of the crystal parameters and the supply voltage V_{DD}.

Chapter 4

Minimalisation of the start-up energy

In this chapter the influence of the different design parameters on the total start-up energy will be investigated. This will be done by performing numerical calculations in Matlab. For these calculations a certain crystal is assumed. The parameters of this crystal are given in table 4.1. These crystal parameters are just used as an example. Of course the analysis can also be applied for other crystal parameters.

Table 4.1: Specified crystal parameters [1]

Parameter	Value
L_M	$11.1mH$
C_M	$3.96fF$
R_M	19Ω
f_0	$24MHz$
C_S	$2pF$
C_L	$6pF$

4.1 Dependence of R_{N3} on C_{o1} and C_{o2}

As already became clear, the size of the capacitors C_{o1} and C_{o2} determines how inductive the impedance Z_{amp-3} will be. In order to get an idea of the region in which Z_{amp-3} is inductive, $Im(Z_{amp-3})$ is plotted for different values of C_{o1} and C_{o2}, while the other parameters are fixed. Figure 4.1(c) shows a surface plot of $Im(Z_{amp-3})$ versus C_{o1} and C_{o2}, when the other parameters are fixed at constant values. From this plot it becomes clear that in a certain range of C_{o1} and C_{o2}, $Im(Z_{amp-3})$ is bigger than zero (i.e. inductive). In order to get a better picture for which values of C_{o1} and C_{o2} $Im(Z_{amp-3})$ is inductive, a contour plot is made, which can be found in figure 4.1(d). From this plot it follows that for the given parameters, $Im(Z_{amp-3})$ is inductive between $C_{o1} = C_{o2} \approx 0.2pF$ and $C_{o1} = C_{o2} \approx 2pF$.

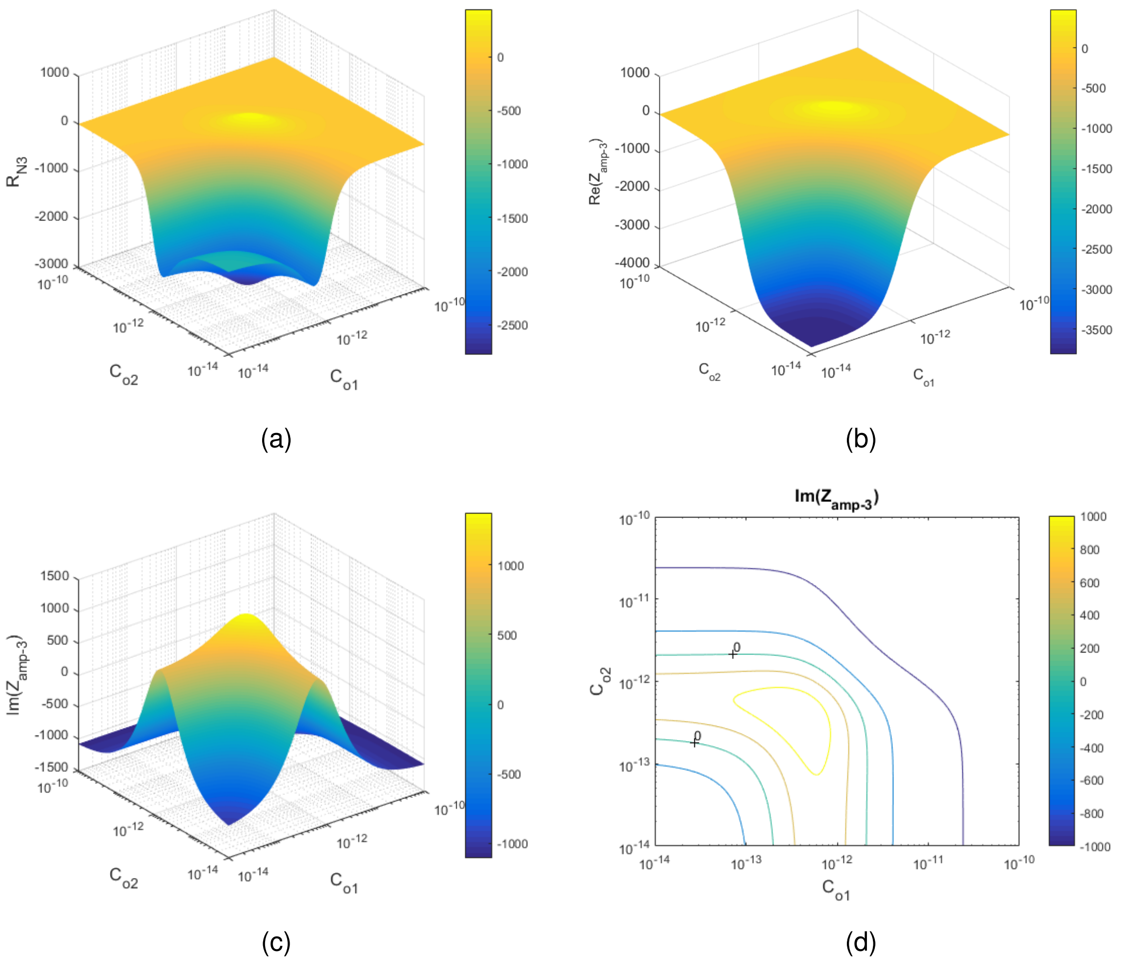

Figure 4.1: Effect of varying C_{o1} and C_{o2} on: (a) R_{N3}; (b) $Re(Z_{amp-3})$; (c) $Im(Z_{amp-3})$; and, (d) contour plot of $Im(Z_{amp-3})$; when $R_{inv1} = R_{inv2} = 10k\Omega, g_{m1} = g_{m2} = g_{m3} = 0.5mS, f = 24MHz, C_S = 2pF$ and $C_L = 6pF$

Table 4.2: Values for C_{o1} and C_{o2} which result in the optimum values for R_{N3} and $Im(Z_{amp-3})$

	C_{o1} $[pF]$	C_{o2} $[pF]$
Minimum R_{N3}	0.35	0.35
Maximum $Im(Z_{amp-3})$	0.38	0.38

As was already mentioned, Z_{amp-3} should be inductive in order to optimize the value of R_N. Figure 4.1(a) shows a surface plot in which R_{N3} is plotted against C_{o1} and C_{o2}. When comparing figure 4.1(c) with figure 4.1(a), it becomes clear that R_{N3} has indeed a minimum in the same region as where $Im(Z_{amp-3})$ has a maximum. To check if the minimum for R_{N3} occurs at exact the same values for C_{o1} and C_{o2} as where $Im(Z_{amp-3})$ has a maximum, the coordinates of C_{o1} and C_{o2} are determined. The results are given in table 4.2. From this table it becomes clear that the minimum of R_{N3} and the maximum of $Im(Z_{amp-3})$ appear when the values of C_{o1} and C_{o2} are equal. Also when checking this for different values of the other parameters, this appears to be the case. Because of this, R_{N3} and $Im(Z_{amp-3})$ can also be calculated by varying only C_o, in which $C_o = C_{o1} = C_{o2}$. This will reduce the computational complexity of the calculations that will be performed later on in this chapter.

Another thing that can be concluded from table 4.2 is that the minimum value for R_{N3} does not exactly occur at the same values for C_{o1} and C_{o2} as where $Im(Z_{amp3})$ has a maximum. This is caused by the fact that the optimum value of R_{N3} does not only depend on $Im(Z_{amp3})$, but also on $Re(Z_{amp-3})$. When $Re(Z_{amp-3})$ becomes smaller, R_{N3} will become bigger, which can also be seen in equation 2.6. From this equation it follows that $Re(Z_{amp-3})$ only contributes by a power of 1 to the numerator, while it contributes with a power of 2 to the denominator, which causes R_{N3} to increase when $Re(Z_{amp-3})$ decreases. Figure 4.1(b) shows a surface plot in which $Re(Z_{amp-3})$ is plotted for different values of C_{o1} and C_{o2}. From this plot it follows that $Re(Z_{amp-3})$ increases when the values of C_{o1} and C_{o2} are increased.

In order to get a better insight in how $Im(Z_{amp-3})$ and $Re(Z_{amp-3})$ influence the value of the negative resistance R_{N3}, a 2D plot is made in which R_{N3}, $Im(Z_{amp-3})$ and $Re(Z_{amp-3})$ are plotted against C_o, in which $C_o = C_{o1} = C_{o2}$. This plot can be found in figure 4.2. From this plot it becomes clear that the minimum value for R_{N3} (i.e. the optimum value of R_{N3}) appears indeed at a slightly smaller value of C_o as where $Im(Z_{amp-3})$ has its maximum. This is caused by the fact that $Re(Z_{amp-3})$ decreases for smaller values of C_0, which can also be seen in figure 4.2.

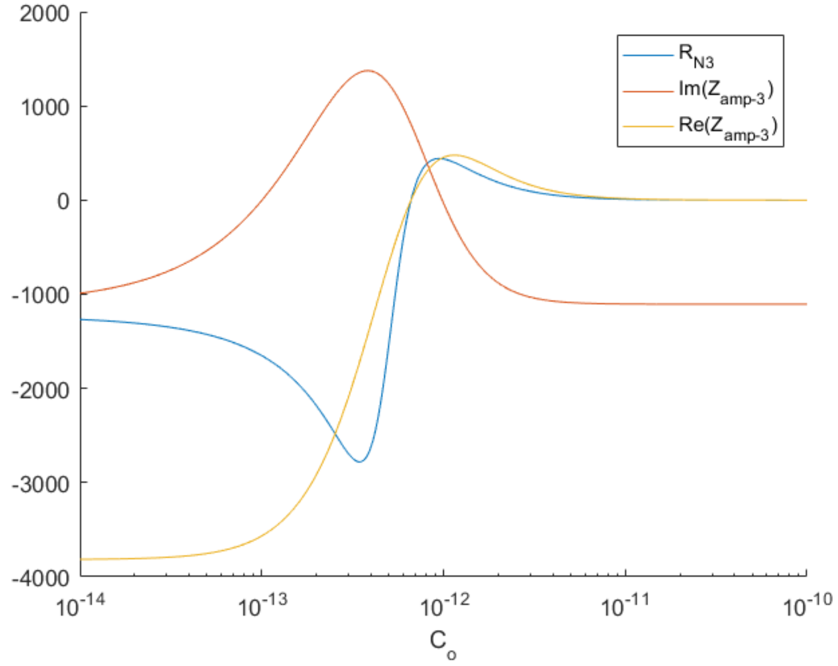

Figure 4.2: Plot of R_{N3}, $Im(Z_{amp-3})$ and $Re(Z_{amp-3})$ versus C_o, for $R_{inv1} = R_{inv2} = 10k\Omega, g_{m1} = g_{m2} = g_{m3} = 0.5mS, f = 24MHz, C_S = 2pF$ and $C_L = 6pF$

4.2 Influence of R_{inv} on optimum R_{N3}

In section 4.1 the influence of C_{o1} and C_{o2} on R_{N3} was evaluated for a fixed value of R_{inv}. This resulted in an optimum value for R_{N3}, as given in the plot of figure 4.1(a). When looking to this plot, the question can be asked how this maximum of R_{N3} can be increased further by adjusting the other parameters. However, when the other parameters are adjusted, this may also result in another optimum value for R_{inv}. In this section it will be evaluated what the influence of R_{inv} is on the optimum values for C_{o1} and C_{o2}, and how this affects the maximum value of R_{N3}. First of all R_{inv} is increased from $10k\Omega$ to $13k\Omega$. This results in the plot of figure 4.3. When looking to this plot it can be concluded that the same behavior is observed as in figure 4.1(a), but that the optimum value of R_{N3} has increased. This is indeed a logical result, because increasing the total resistance of an inverter stage will also increase the gain, according to equation 3.5. Table 4.3 gives a comparison between the values of R_{N3}, C_{o1} and C_{o2} for $R_{inv} = 10k\Omega$ and $R_{inv} = 13k\Omega$.

From the results mentioned in table 4.3 it can be concluded that increasing the resistance has a positive effect on R_{N3}. The question that arises from these results is if there is a limit of increasing the value of the resistance, after which it does not have a positive effect anymore. In order to find an answer to this question, the simulation which resulted in the plot of figure 4.3 will be executed multiple times for

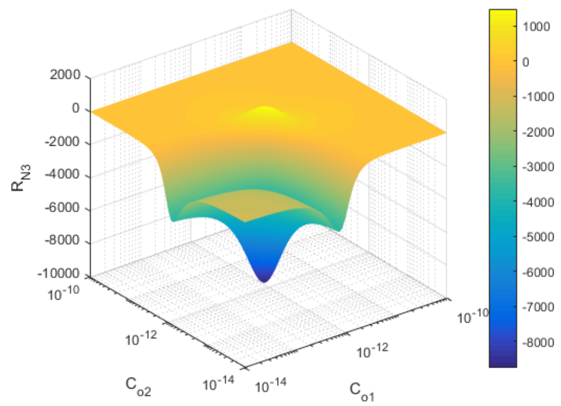

Figure 4.3: Surface plot of R_{N3} versus C_{o1} and C_{o2} for $R_{inv} = 13k\Omega, g_{m1} = g_{m2} = g_{m3} = 0.5mS, f = 24MHz, C_S = 2pF$ and $C_L = 6pF$

Table 4.3: Comparison of optimum for R_{N3}, C_{o1} and C_{o2} for different values of R_{inv}. $g_{m1} = g_{m2} = g_{m3} = 0.5mS, f = 24MHz, C_S = 2pF$ and $C_L = 6pF$

	$R_{inv} = 10k\Omega$	$R_{inv} = 13k\Omega$
Optimum R_{N3}	$-2.8k\Omega$	$-8.8k\Omega$
Optimum C_{o1}	$0.34pF$	$0.41pF$
Optimum C_{o2}	$0.34pF$	$0.41pF$

different values of R_{inv}. Every time this simulation is executed, the minimum value for R_{N3} will be determined when varying C_{o1} and C_{o2}. However, as already observed in the previous section, the minimum value for R_{N3} occurs for equal values of C_{o1} and C_{o2}. Therefore the simulations will be performed by only varying C_o, in which $C_o = C_{o1} = C_{o2}$. In this way the minimum value of R_{N3} is found with respect to C_o for different values of R_{inv}. This means that for every value of R_{N3}, the optimum value of C_o is chosen such that the minimum value of R_{N3} is achieved. Figure 4.4 shows a plot in which the minimum of R_{N3} is plotted for different values of R_{inv}. Furthermore this plot shows the maximum value of R_{N3} for the same values of R_{inv}.

From figure 4.4 it can be concluded that after R_{inv} has reached a value of around $15k\Omega$, the minimum value of R_{N3} goes to minus infinity. However, from this plot it also follows that when R_{inv} increases by a small amount, the maximum value of R_{N3} can go to plus infinity. To get a better idea of the stability of the oscillator for certain values of R_{inv} and C_o, the values of C_o that result in the minimum and maximum R_{N3} are plotted for different values of R_{inv}. The result is given in figure 4.6. From figure 4.6 it can be concluded that when increasing R_{inv}, the values of $C_{o,opt}$ that result in the minimum and maximum R_{N3} get closer to each other, and at the point where $C_{o,opt}$ has a peak, the value of $C_{o,opt}$ that results in the minimum R_{N3} is almost equal

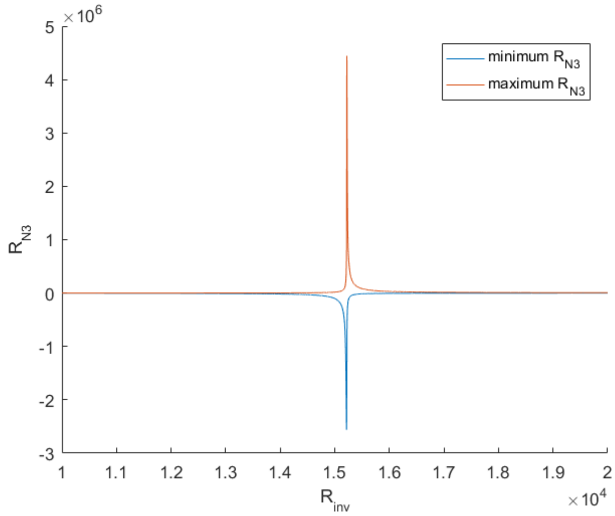

Figure 4.4: Plot of minimum and maximum values of R_{N3} versus R_{inv}, for $g_{m1} = g_{m2} = g_{m3} = 0.5mS, f = 24MHz, C_S = 2pF$ and $C_L = 6pF$

to the value of $C_{o,opt}$ that results in the maximum R_{N3}. In figure 4.7 the difference in capacitance value is plotted that result in the maximum value of R_{N3} and the minimum value of R_{N3} (i.e. the difference between the red curve and the blue curve of figure 4.6). When calculating the minimum of this curve, a value of approximately $0.4fF$ is obtained. In reality this accuracy in capacitance can never be reached, because when the capacitance values become very small, parasitic capacitances will start to play a role. An example of such a parasitic capacitance is the gate drain capacitance. For the used MOSFET, this capacitance is determined, and its value appeared to be $2.67fF$. This value is already much bigger than the difference of $0.4fF$ which causes the R_{N3} to change from a very big negative value to a very big positive value. Also external factors like temperature variations can cause small changes in the capacitance value.

In order to ensure that the value of the negative resistance of the oscillator cannot become (infinitely) positive, the optimum value of R_{N3} should be chosen somewhere on the curve before R_{N3} has reached minus infinity. This point can be chosen based on the application for which the oscillator is going to be used. In order to give a measure how close the value of R_{N3} is with respect to minus infinity, the derivative of the blue curve in figure 4.4 can be taken (i.e. the derivative of R_{N3} with respect to R_{inv}). This results in the plot shown in figure 4.5. The derivative gives an indication how sensitive the value of R_{N3} is for variations in parameter values. When the derivative is smaller, the sensitivity of R_{N3} to variations in the resistance R_{inv} decreases. This reduces the chance that the negative resistance becomes positive. Furthermore a smaller derivative means that R_{inv} decreases (as long as you stay left of the blue curve in figure 4.4). When R_{inv} decreases, the difference between the values of

$C_{o,opt}$ that result in the minimum and maximum R_{N3} increases, as can be seen in figure 4.6. Therefore the robustness of R_{N3} for variations in C_o also increases when the derivative of R_{N3} with respect to R_{inv} decreases. Furthermore, the transconductance does not have a direct effect on the stability of R_{N3}, since it only changes the value of R_{inv} for which the peak in R_{N3} occurs. This will become clear in section 4.3.

The value of the derivative can be chosen based on the kind of application for which the oscillator is going to be used. If for example the oscillator has to operate in an area in which the temperature can fluctuate a lot, the derivative should be chosen smaller. This reduces the chance that the negative resistance becomes infinitely high due to small variations in parameter values when the temperature changes.

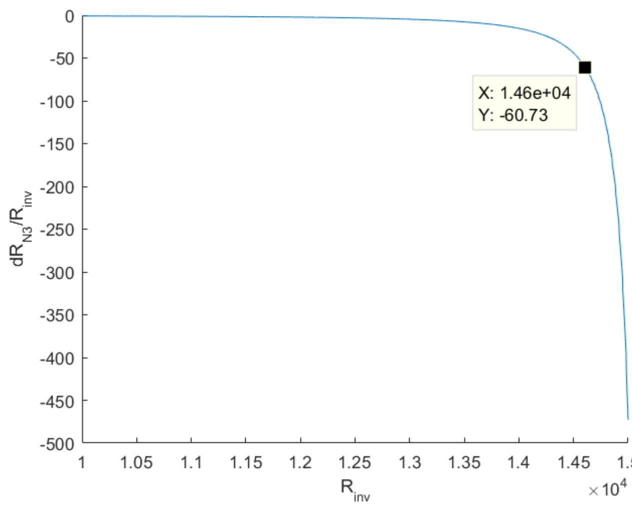

Figure 4.5: Plot of derivative of optimum R_{N3} with respect to R_{inv}, for $g_{m1} = g_{m2} = g_{m3} = 0.5mS, f = 24MHz, C_S = 2pF$ and $C_L = 6pF$

In order to explain the behavior of the negative resistance in the plot of figure 4.4, the real and imaginary part of Z_{amp-3} that correspond to the minimum value of R_{N3} in figure 4.4 are plotted against R_{inv}. The results can be found in figure 4.8 and 4.9, respectively. In figure 4.9 an additional red line is plotted. This line represents the value for $Im(Z_{amp-3})$ for which the second term in the denominator of equation 2.6 becomes exactly zero (i.e. the stray capacitance is fully compensated by the inductance generated by $Im(Z_{amp-3})$). This condition is also given in equation 4.1:

$$Im(Z_{amp-3}) = \frac{1}{\omega_0 C_S} \tag{4.1}$$

When comparing figure 4.4 with figure 4.9 it becomes clear that at the point where R_{N3} is minimum, the imaginary part of Z_{amp-3} is exactly equal to the condition presented in equation 4.1 (which is represented by the red line in figure 4.9). Furthermore, when looking to figure 4.8 it can be concluded that at this point the

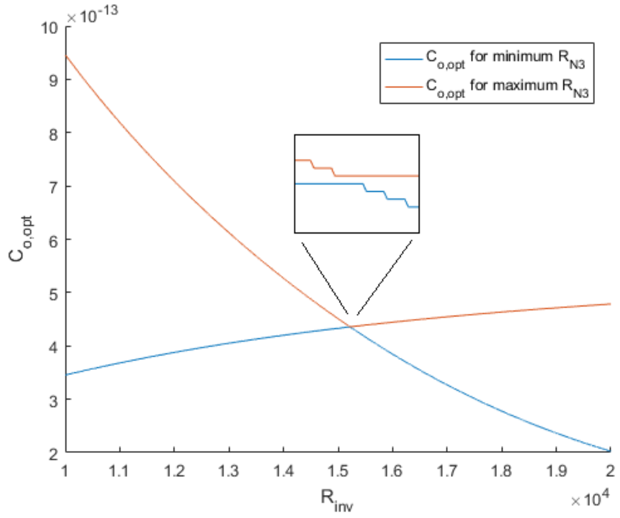

Figure 4.6: Plot of C_o that results in minimum and maximum values of R_{N3} versus R_{inv}, for $g_{m1} = g_{m2} = g_{m3} = 0.5mS, f = 24MHz, C_S = 2pF$ and $C_L = 6pF$

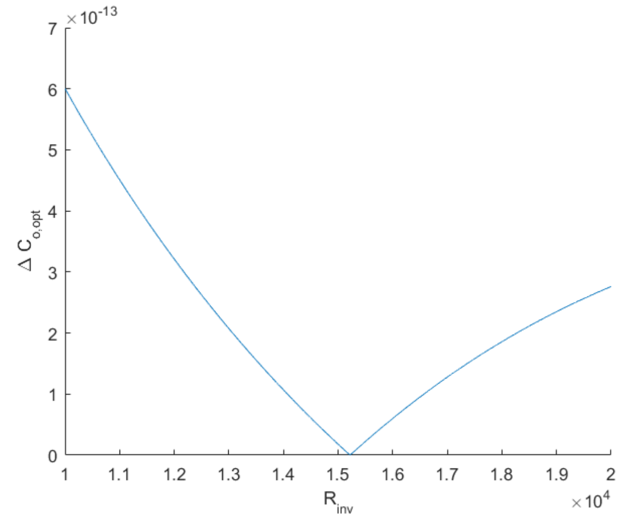

Figure 4.7: Plot of difference in value of $C_{o,opt}$ versus R_{inv}, for $g_{m1} = g_{m2} = g_{m3} = 0.5mS, f = 24MHz, C_S = 2pF$ and $C_L = 6pF$

optimum real part of Z_{amp-3} is almost equal to zero. This is indeed a logical result, because when the imaginary part of Z_{amp-3} exactly cancels the stray capacitance, equation 2.6 becomes:

$$R_N = \frac{Re(Z_{amp})}{(\omega_0 C_S Re(Z_{amp}))^2} \tag{4.2}$$

Which can be rewritten to:

$$R_N = \frac{1}{(\omega_0 C_S)^2 Re(Z_{amp})} \tag{4.3}$$

From this equation it becomes clear that R_{N3} grows towards infinity when $Re(Z_{amp-3})$ approaches zero, in which zero is the asymptote. Therefore, when $Im(Z_{amp-3})$ exactly cancels the impedance of the stray capacitance at the resonance frequency, R_{N3} can become infinite. This is the reason why the peak in figure 4.4 goes towards infinity for a certain value of R_{inv}.

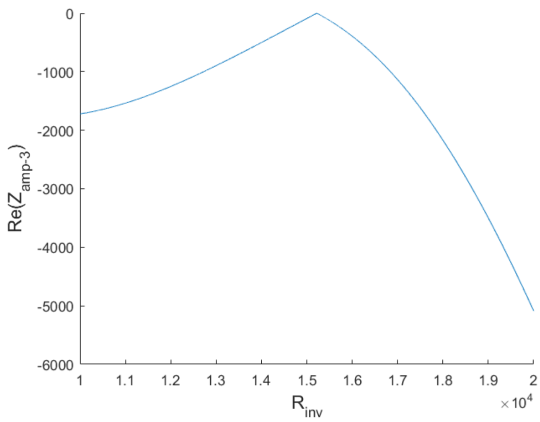

Figure 4.8: $Re(Z_{amp-3})$ that corresponds with minimum for R_{N3} when varying R_{inv}, for $g_{m1} = g_{m2} = g_{m3} = 0.5mS, f = 24MHz, C_S = 2pF$ and $C_L = 6pF$

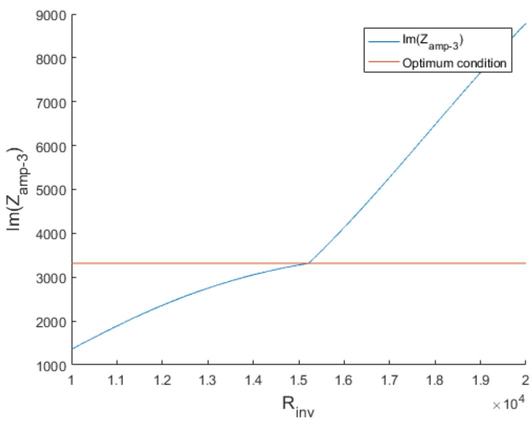

Figure 4.9: $Im(Z_{amp-3})$ that corresponds with minimum for R_{N3} when varying R_{inv}, and indication of condition that results in optimum $Im(Z_{amp-3})$. For $g_{m1} = g_{m2} = g_{m3} = 0.5mS, f = 24MHz, C_S = 2pF$ and $C_L = 6pF$

4.3 Influence of g_m on optimum R_{N3}

In the previous sections the influence of C_o and R_{inv} on the negative resistance was evaluated. This resulted in an optimum for R_{N3} as a function of R_{inv}. In this section it will be investigated which influence the transconductance g_m has on this optimum for R_{N3}. In order to do this, the g_m of each inverter stage is increased from $0.5mS$ to $0.6mS$. The result is given in figure 4.10. From this figure it becomes clear that when varying g_m, the optimum value of R_{inv} changes. More specifically, when increasing g_m from $0.5mS$ to $0.6mS$, the optimum value of R_{inv} decreases from approximately $15k\Omega$ to approximately $11.5k\Omega$. This is a logical result, because both in the real and the imaginary part of Z_{amp-3} g_m is multiplied with R_{inv} (see equation 3.2), so when g_m increases, R_{inv} should decrease in order to keep the (same) optimum value.

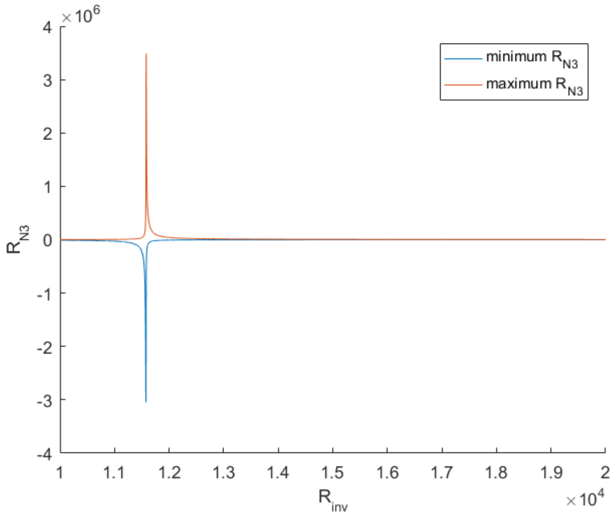

Figure 4.10: Plot of minimum and maximum values of R_{N3} versus R_{inv}, for $g_{m1} = g_{m2} = g_{m3} = 0.6mS, f = 24MHz, C_S = 2pF$ and $C_L = 6pF$

4.4 Minimizing the start-up energy

In the previous sections the influence of the individual parameters on the negative resistance was investigated. In this section all this knowledge will be put together in order to find the parameters that result in the minimum start-up energy. As was discussed in section 4.2, the negative resistance can theoretically become infinitely small (i.e. minus infinity) if exact the right values for the different parameters are chosen. However, in section 4.2 it was also demonstrated that a small change in C_o or R_{inv} can result in a negative resistance that becomes infinitely big (i.e. plus infinity). Because of this, a value of the negative resistance can be chosen some-

Table 4.4: Specifications of $0.36\mu m$ NMOS transistor

Parameter	Value
V_{TH}	$0.58V$
μC_{OX}	$2.75mA/V^2$
W	$3.6\mu m$
L	$0.36\mu m$
λ	$0.0447V^{-1}$

where on the curve of figure 4.4 before it reaches minus infinity. In order to indicate how far the negative resistance is from the point where it becomes minus infinity, the derivative of R_{N3} can be taken with respect to R_{inv}, as was demonstrated in section 4.2. The closer the negative resistance gets to minus infinity, the bigger this derivative will be. For the remainder of this chapter it will be assumed that this derivative is equal to 60 (see figure 4.5). This value is just used as an example. As already mentioned in section 4.2, the value of the derivative can be chosen based on the kind of application for which the oscillator is going to be used.

For the calculations that are performed in this section, a certain NMOS is assumed with fixed parameters. The parameters of the NMOS can be found in table 4.4. Of course, the same analysis can be performed for different MOSFET parameters.

The steps below give the main aspects of the approach that is used to find the circuit parameters that result in the minimum start-up energy. Some of these steps refer to equations that are needed in order to perform that step. Most of these equations are already explained in the previous chapters of this report. The other equations that are used will be explained in more detail after the description of the steps is finished.

1. g_m is varied over a certain range. This range can be chosen based on the application for which the crystal oscillator is going to be used. In this research the range is varied from $g_m = 10\mu S$ to $g_m = 1mS$.

2. For every value of g_m, R_{inv} is varied over a certain range. This range should be chosen in such a way that for every value of g_m the optimum value of R_{inv} can be chosen.

3. For every value of g_m and R_{inv}, C_o is varied over a certain range, and for every value of C_o, R_{N3} is calculated. Again this range of C_o should be chosen sufficiently big. However, the lowest value of this range should not be too small in order to prevent unwanted effects caused by the parasitic capacitances of the MOSFET.

4. When R_{N3} is calculated for every value of C_o, the minimum value of R_{N3} is determined and stored in an array.

5. This process is repeated for the complete range of R_{inv}.

6. Next the derivative of R_{N3} is taken with respect to R_{inv}. As already mentioned in the beginning of this section a derivative of 60 is assumed. This derivative defines how close the value of R_{N3} is to the point where it is minus infinity, and gives therefore information about the robustness of R_{N3} for parameter variations.

7. Based on the derivative, the corresponding value of R_{inv} is determined.

8. Next the drain current is calculated from the value of g_m using equation 4.7.

9. Based on the drain current, the output resistance of the MOSFETs is calculated using equation 4.8.

10. Next the value of the drain resistor is calculated based on the value of R_{inv} and the output resistance of the MOSFET using equation 4.10.

11. Furthermore the start-up time is calculated using the different equations described in section 3.4.

12. Finally, the total start-up energy is calculated based on the supply voltage V_{DD}, the drain current I_D and the start-up time, according to equation 3.4.

13. Step 2 till 12 are repeated for every value of g_m.

The steps above give a general overview of the process of determining the minimum start-up energy. For the exact implementation of these steps the Matlab code can be consulted.

The Matlab code contains different equations in order to calculate the different parameters. For example, the drain current has to be calculated from the value of the transconductance (g_m), as is indicated in step 8. In order to do this, a relation between the g_m and the drain current is needed. This relation can be derived when considering the equations for the transconductance and the drain current. The transconductance is defined as follows:

$$g_m = \mu C_{OX}\frac{W}{L}(V_{GS} - V_{TH}) \tag{4.4}$$

Furthermore, the drain current when the MOSFET is in saturation is defined as:

$$I_D = \frac{1}{2}\mu C_{OX}\frac{W}{L}(V_{GS} - V_{TH})^2 \tag{4.5}$$

Equation 4.4 and 4.5 can be rewritten such that $V_{GS} - V_{TH}$ is expressed as a function of g_m and I_D, respectively. In this way an expression for g_m can be derived as a function of I_D. When performing the required calculations, the following result is obtained:

$$g_m = \sqrt{2\mu_n C_{OX} \frac{W}{L} I_D} \tag{4.6}$$

However, during the simulation g_m is sweeped, so in order to calculate I_D, I_D should be defined as a function of g_m. When rewriting equation 4.6 this results in:

$$I_D = \frac{g_m^2}{2\mu_n C_{OX} \frac{W}{L}} \tag{4.7}$$

After the drain current has been determined, the output resistances of the MOSFETS can be calculated. The relation between the drain current and the output resistance of the MOSFET is given by equation 4.8:

$$r_o = \frac{1}{\lambda I_D} \tag{4.8}$$

During the simulation the total small signal resistance of the inverter R_{inv} is sweeped for every value of g_m. For small signals the output resistance of the inverter r_o is connected in parallel with the drain resistor R_D. Therefore, the total small signal resistance of each inverter stage is given by:

$$R_{inv} = R_D // r_o = \frac{R_D r_o}{R_D + r_o} \tag{4.9}$$

As already mentioned, during the simulations R_{inv} will be swept. Therefore R_D can be calculated using R_{inv} and the previously found value for r_o. In order to calculate R_D, equation 4.9 can be rewritten to:

$$R_D = -\frac{R_{inv}}{R_{inv}\lambda I_D - 1} \tag{4.10}$$

4.4.1 Simulation results

After running the calculation, the plot of figure 4.11 is obtained, which shows the total start-up energy as a function of the transconductance g_m. From this plot it becomes clear that the total start-up energy decreases when g_m decreases. However, from this plot it also follows that at a g_m of $40\mu S$, the start-up energy increases again. This is caused by the fact that the lower limit of the range values over which C_o is varied is set to $10fF$, while for low values of g_m, the optimum C_o is below $10fF$. Figure 4.14(c) shows the graph in which the optimum value of C_o is plotted versus g_m. In this plot it can be seen that at a g_m of $40\mu S$ the value of C_o has reached its lower limit of $10fF$.

When this limit is reached, the optimum value of C_o cannot be chosen anymore, and therefore the start-up energy increases for a value of g_m smaller than or equal to $40\mu S$, as can be seen in the plot of figure 4.11. It can be decided to decrease the lower bound of the range over which the values of C_o are varied. However, in section 4.2 the value of the gate-source capacitance was derived, and it was determined that this value is approximately $2.67fF$. This means that when decreasing the lower bound of the range of C_o, the value of this capacitance will start to play a significant role. Therefore the value of g_m should not be chosen smaller than or equal to $40\mu S$. When this is however done, the parasitic capacitances of the MOSFET should be taken into account.

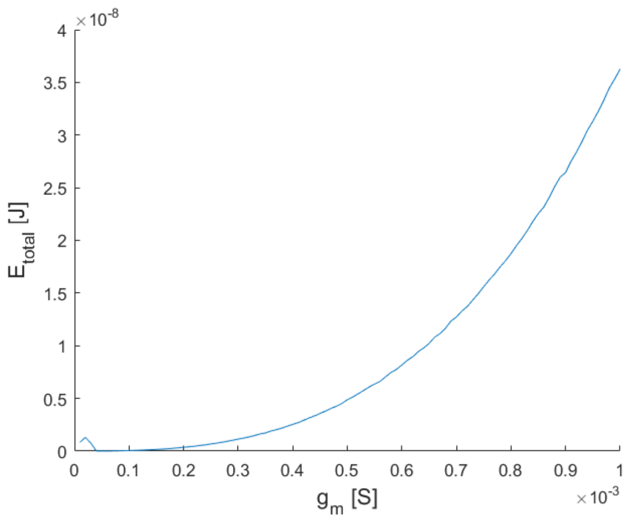

Figure 4.11: Start-up energy as a function of g_m for a gradient of 60; $f = 24MHz, C_S = 2pF$ and $C_L = 6pF$

In order to analyze the behavior of the total start-up energy, it is interesting to see what the influence of the negative resistance is on the total start-up energy. Figure 4.12 shows a plot of the negative resistance as a function of g_m. From this plot it can be concluded that the negative resistance decreases rapidly when increasing the value of g_m. This is also what is expected when looking to the plot of the total start-up energy (see figure 4.11), in which it is visible that the total start-up energy increases rapidly when increasing the g_m. However, the start-up energy is not only determined by the negative resistance. Also the drain current plays an important role in the total energy consumption. In figure 4.13 the drain current is plotted against g_m. From this plot it follows that the drain current increases quadratically when increasing g_m. This directly follows from equation 4.7.

In the plot of the negative resistance it becomes clear that the negative resistance has a minimum at a g_m of $50\mu S$. The reason that the negative resistance increases again for smaller values of g_m is caused by the fact that the value of C_o is not correct

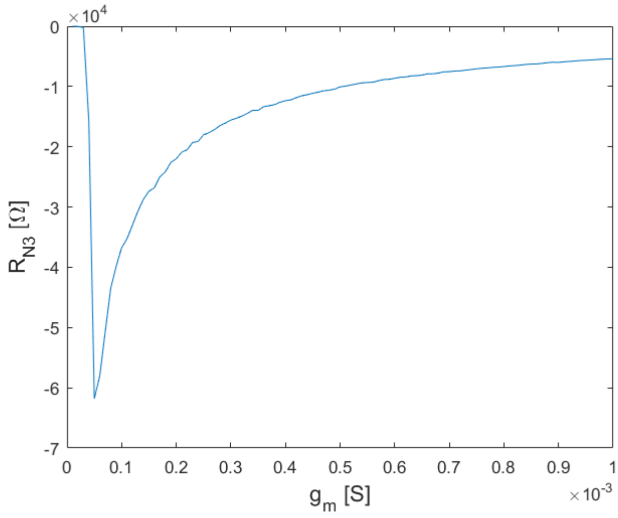

Figure 4.12: R_{N3} as a function of g_m for a gradient of 60; $f = 24MHz, C_S = 2pF$ and $C_L = 6pF$

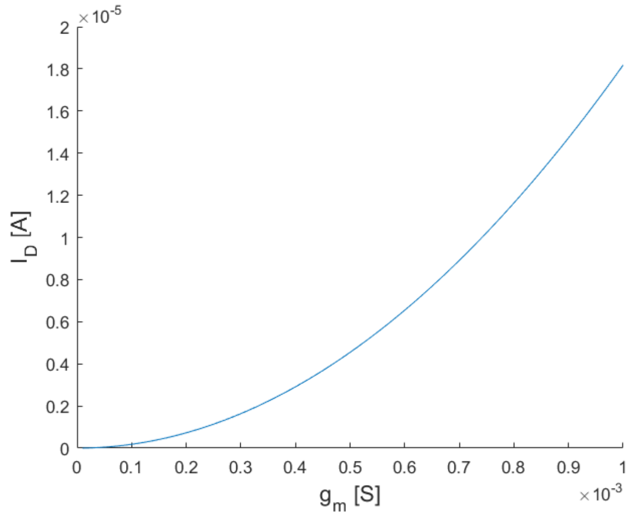

Figure 4.13: Drain current as a function of g_m for a gradient of 60; $f = 24MHz, C_S = 2pF$ and $C_L = 6pF$

anymore for values of g_m smaller than or equal to $40\mu S$, as already became clear in the beginning of this section. Another thing that should be noted is that the value of R_{N3} that is plotted in figure 4.12 is not the optimum value of R_{N3}, but the value of R_{N3} at the point where its derivative with respect to the total small signal inverter resistance R_{inv} is equal to 60. The optimum negative resistance that is achieved in this way is $-61k\Omega$ for $g_m = 50\mu S$, as can be seen in table 4.5. In this table the optimum parameters are given for a g_m of $50\mu S$.

From the plot of figure 4.11 it follows that the total start-up energy decreases when decreasing g_m. On the one hand this is a logical result, because increasing

Table 4.5: Optimum parameters for a g_m of $50\mu S$

Minimum start-up energy	$7.95pJ$
Corresponding parameters	
R_{N3}	$-61.8k\Omega$
g_m	$50\mu S$
R_D	$470k\Omega$
r_o	$492M\Omega$
C_o	$13.7fF$
I_D	$1.5\mu A$
V_{DD}	$5V$
t_s	$9.04\mu s$

the g_m means that the drain current also increases (according to equation 4.7), and therefore the total start-up energy increases. On the other hand decreasing the g_m would also result in a lower gain, which would increase the start-up time and therefore increase the start-up energy. However, a high gain can also be achieved by increasing the total small signal resistance R_{inv} of every inverter, as already became clear from equation 3.5. In order to get an idea of the value of R_{inv} for different values of g_m, R_D and r_o are plotted as a function of g_m in figures 4.14(a) and 4.14(b), respectively. From these figures it becomes clear that R_D and r_o indeed increase when g_m decreases. This is as expected, because a big value of R_D and r_o still allows a high gain, even when the g_m is low.

Another thing that can be noted in the plot of R_D in figure 4.14(a) is that at a certain point R_D reaches a maximum. The g_m for which this maximum occurs is exactly at $40\mu S$, which is also the point after which the optimum value of C_o cannot be achieved anymore. Therefore the results of R_D are not valid anymore for values of g_m smaller than $40\mu S$.

Another thing that becomes clear from the plot in figure 4.14(a) is that the optimum value of R_D becomes rather small when g_m increases. For example, at a g_m of $1mS$ the optimum value of R_D is approximately $4.23k\Omega$. When such a small value of R_D is chosen, the impedance of this resistance gets in the same order of magnitude as the impedance of the load capacitance C_{P2} (which is $2C_L$). In this case the resistance R_{inv3} (i.e. the total small signal resistance of the third inverter) cannot be neglected anymore in the equation for R_{N3}. For high values of R_D, the phase shift generated by the parallel RC combination is approximately $-89°$, while the phase shift becomes approximately $-82.6°$ for a drain resistance of $4.23k\Omega$. Therefore it

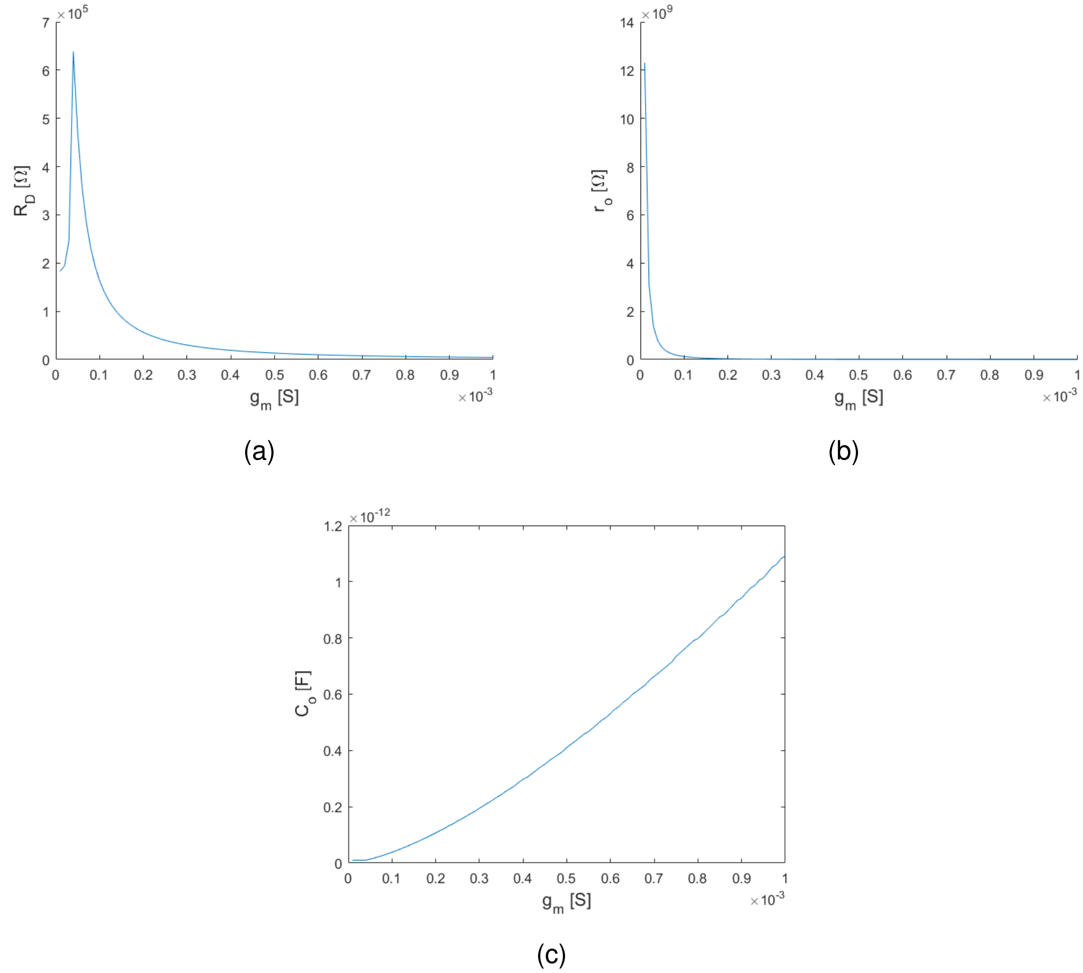

Figure 4.14: Circuit parameters resulting in the minimum start-up energy: (a) R_D as a function of g_m; (b) r_o as a fucntion of g_m; and, (c) C_o as a function of g_m; for $f = 24MHz, C_S = 2pF$ and $C_L = 6pF$.

can be concluded that for small values of the drain resistance, this resistance should be incorporated in the equation for R_{N3}.

Another important parameter is the capacitive load after the first and the second inverter stage (C_{o1} and C_{o2}). Figure 4.14(c) shows a plot of the optimum value of C_o as a function of g_m (in which $C_o = C_{o1} = C_{o2}$). In the beginning of this section the behaviour of the output capacitances was already analyzed for small values of g_m. For big values of g_m it can be observed in the plot of figure 4.14(c) that C_o increases for increasing g_m. This is indeed a logical result, because an increase in g_m means that the drain current also increases. When the drain current becomes higher, bigger capacitors are needed in order to keep the same voltage over the capacitors.

In this section the optimum design parameters are investigated for a certain 'safety margin' (i.e. the derivative of 60). It became clear that the start-up energy decreases for decreasing values of g_m. However, for a g_m of around $40\mu S$ parasitic effects of the MOSFETS will start to play a significant role. Therefore the optimum design parameters are determined for a g_m of $50\mu S$. These optimum parameters can be found in table 4.5. In the next section it will be evaluated if these results of the three-stage inverter implementation are indeed better than the results that are obtained for the single-stage inverter implementation.

4.5 Minimum energy consumption for single inverter circuit

In this section the optimum value of g_m will be investigated that results in the minimum start-up energy for the single stage inverter crystal oscillator. In chapter 2 already an expression for the minimum value of R_{N1} was given [1]:

$$R_{N1,min} = -\frac{C_L}{2\omega_0 C_S(C_L + C_S)} \tag{4.11}$$

For the crystal that is considered in this chapter (see table 4.1), this minimum value of R_{N1} can be calculated as follows:

$$R_{N1,min} = -\frac{6 \cdot 10^{-12}}{2 \cdot 2\pi \cdot 24 \cdot 10^{6} \cdot 2 \cdot 10^{-12}(6 \cdot 10^{-12} + 2 \cdot 10^{-12})} \approx -1243k\Omega \tag{4.12}$$

The value of g_m for which this minimum for R_{N1} occurred was also given in chapter 2 [1]:

$$g_m = 4\omega_0 C_L(1 + \frac{C_L}{C_S}) \tag{4.13}$$

For the given crystal, this value of g_m becomes:

$$g_m = 4 \cdot 2\pi \cdot 24 \cdot 10^{6} \cdot (1 + \frac{6 \cdot 10^{-12}}{2 \cdot 10^{-12}}) \approx 14.5mS \tag{4.14}$$

In order to check these results, the negative resistance is plotted for different values of g_m. The result can be found in figure 4.15. From this figure it can be observed that the minimum value of R_{N1} that can be achieved with the single inverter stage implementation is indeed equal to $-1243k\Omega$. Furthermore it is verified that this minimum does occur at a g_m of $14.5mS$.

In order to see whether this minimum in R_{N1} also results in the minimum start-up energy, the start-up energy is plotted for different values of g_m. The result can be found in figure 4.16.

In this figure the same behavior is observed as in the figure in which the start-up energy of the three-stage inverter implementation is plotted against g_m. It appears

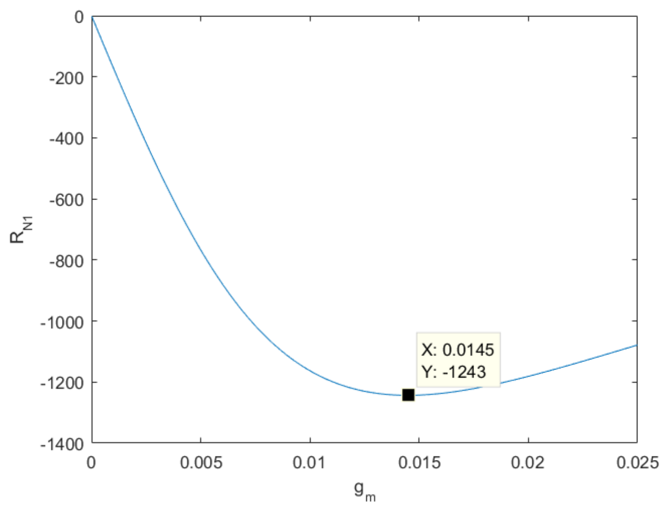

Figure 4.15: R_{N1} as a function of g_m for $f = 24MHz, C_S = 2pF$ and $C_L = 6pF$

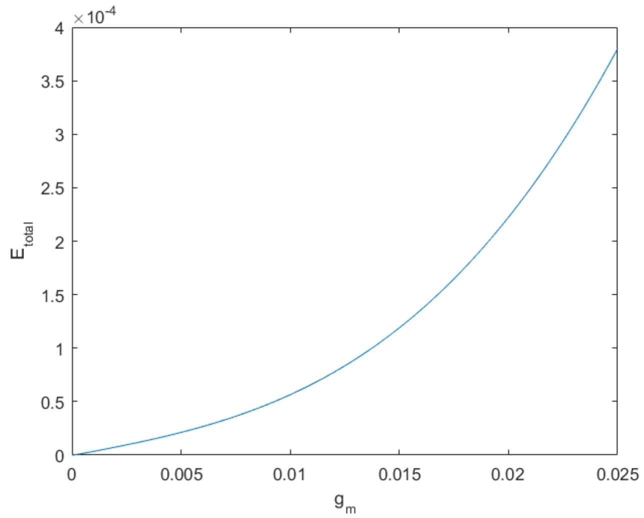

Figure 4.16: Start-up energy of single inverter crystal oscillator as a function of g_m, for $f = 24MHz, C_S = 2pF$ and $C_L = 6pF$

that again the start-up energy decreases when decreasing the value of g_m. It can therefore also be concluded that the minimum start-up energy is not achieved for the minimum value of R_{N1} (which appeared at $g_m = 14.5mS$). In order to make a comparison between the start-up energy of both oscillator circuits, the start-up energy is determined for $g_m = 50\mu S$, which was also done for the three-stage inverter implementation. For this value of g_m, the start-up energy for the single stage inverter implementation is approximately $60.5nJ$. From table 4.5 it follows that for the three-stage inverter implementation the start-up energy is approximately $7,95pJ$. This is about a factor of 7610 lower than the start-up energy of the single-stage inverter crystal oscillator. Therefore it can be concluded that considerable advantages are achieved by using the three-stage inverter crystal oscillator.

Chapter 5

Circuit simulations

In the previous chapter an analysis was given in order to find the optimum design parameters that result in a minimum start-up energy. In this chapter these results will be verified by performing different circuit simulations in LTspice.

5.1 Simulation results for a $\mathbf{g_m}$ of 0.2mS

In the previous chapter it became clear that when the value of g_m decreases, the total start-up energy also decreases. It was also concluded that the optimum values for the output capacitances C_{o1} and C_{o2} decreases, and that therefore parasitic capacitances will start to play a role. Therefore in this section the system will be tested with a g_m that is big enough, such that the influence of parasitic capacitances can be neglected. From the numerical calculations performed in the previous chapter it followed that when for example a g_m of $0.2mS$ is chosen, the optimum value of the output capacitances is approximately given by $C_o \approx 170fF$. This value is sufficiently higher than the value of the parasitic capacitances, which were determined in the previous chapter. Besides the value of the output capacitances of the first two inverter stages, also the values of the other parameters need to be determined. The optimum value of the drain resistors can also be obtained from the numerical calculations performed in chapter 4. The optimum value for the drain resistances for a g_m of $0.2mS$ appeared to be $R_D \approx 56.4k\Omega$.

Before the system will be simulated with a transistor implementation, the system will first be tested by using ideal voltage controlled current sources. In this way any non-linear effects that are introduced by transistors are not present. Also the amplitude of the oscillation will not be limited by the supply voltage. For a g_m of $0.2mS$, this circuit can be found in figure 5.1. Note that in this circuit the value of the resistances R_{inv1} and R_{inv2} is slightly lower than the value of R_D that was mentioned in the previous paragraph. This is because the output resistance of the

MOSFET is taken into account. Because the impedance of the parallel capacitance C_{P2} is sufficiently lower than the impedance of R_{inv3} (which is equal to R_{inv1} and R_{inv2}), R_{inv3} can be neglected. When the voltage across the resonator is plotted for this circuit, the plot of figure 5.2 is obtained. From this plot the amplitude growth coefficient α can be calculated. This amplitude growth coefficient is defined as the inverse of the time constant [5] and therefore gives an indication of the amplitude growth of the signal. The amplitude growth coefficient can be determined using the following equation:

$$\alpha = \frac{ln(A_2) - ln(A_1)}{\Delta t} \tag{5.1}$$

In this equation A_1 and A_2 represent the amplitude of the signal at two different points in time, and Δt is the time difference between these two points. Using this equation, the amplitude growth coefficient is determined for the signal in figure 5.2, and its value appeared to be approximately $975000/s$. The amplitude growth coefficient is also determined from the calculations performed in chapter 4. For a g_m of $0.2mS$, this calculated amplitude growth coefficient appeared to be $991384/s$ (note that the amplitude growth coefficient is the inverse of the time constant, which can be calculated using equation 3.17). This calculated value is approximately the same as the one that is determined from the plot in figure 5.2. The small difference between the calculated growth coefficient and the simulated growth coefficient can be caused by rounding errors for the values of C_o and R_{inv} that were used in the circuit of figure 5.1.

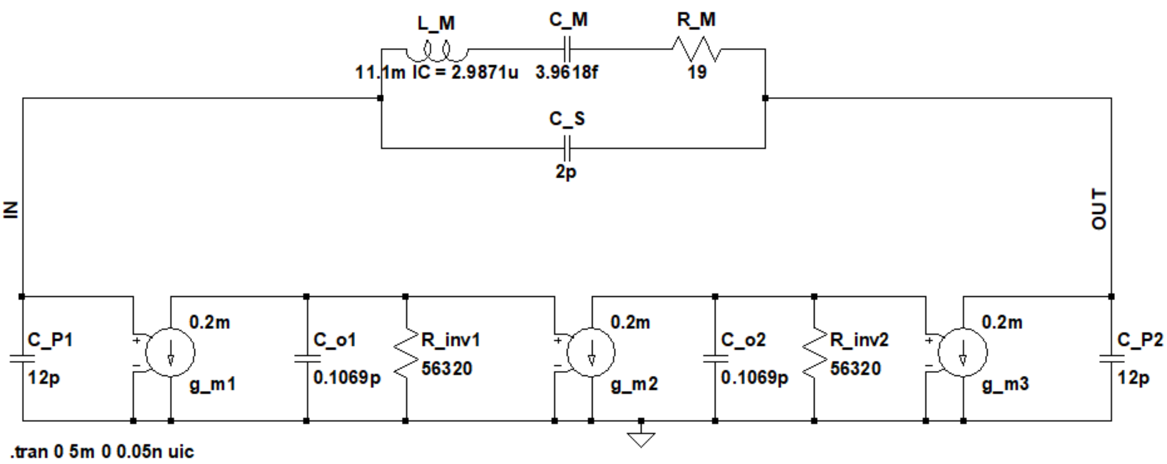

Figure 5.1: Circuit of the three-stage inverter implementation using ideal voltage controlled current sources ($g_m = 0.2mS$)

Next the system will be tested by using the transistor implementation. This will again be done for a g_m of $0.2mS$. As already mentioned, for this value of g_m the

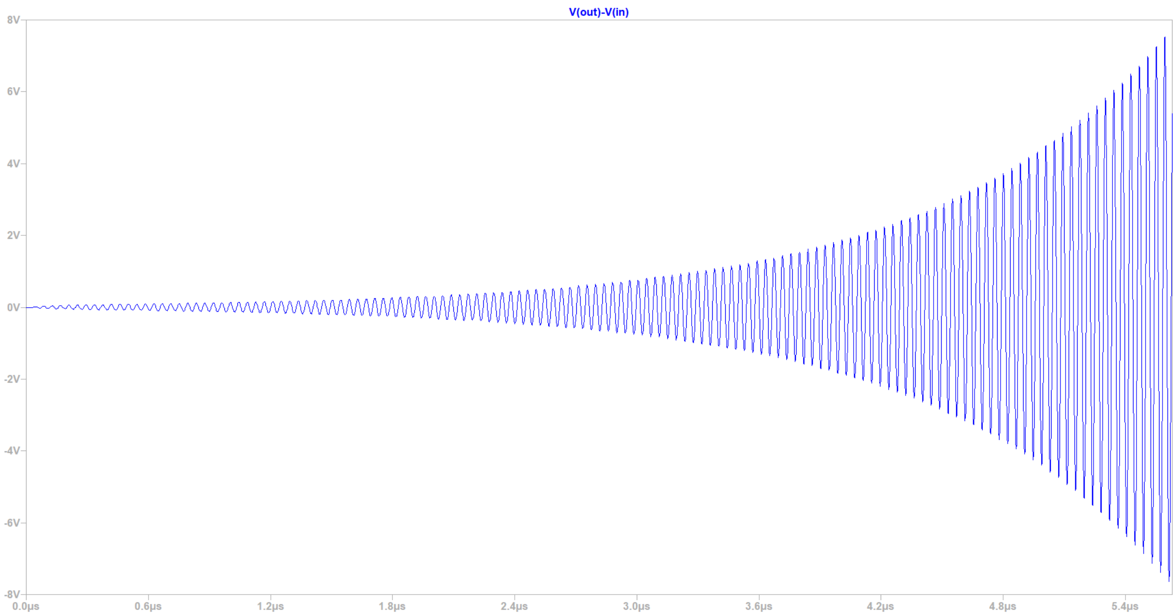

Figure 5.2: Amplitude growth of the voltage across the resonator for the three-stage inverter implementation with ideal voltage controlled current sources ($g_m = 0.2mS$)

calculated optimum value of the output capicatance is given by $C_o \approx 170fF$. Furthermore the calculated optimum value for the drain resistors is $R_D \approx 56.4k\Omega$. The values of the other circuit parameters can be determined based on these parameters. For the bias resistors, a resistance of $200k\Omega$ is chosen, which is sufficiently higher than the defined values of the drain resistors. Next, the values of the coupling capacitors can be calculated. As already mentioned in chapter 3, the values of the coupling capacitors can be calculated using the following equation:

$$C = \frac{1}{2\pi f_{-3dB} R_{eq}} \tag{5.2}$$

Because the MOSFETs have a high input impedance, the equivalent resistance is determined by the value of the bias resistor, which is in this case $200k\Omega$. When substituting the appropriate values in equation 5.2, the following minimum value for the coupling capacitors is obtained:

$$C = \frac{1}{2\pi \cdot 24 \cdot 10^6 \cdot 200 \cdot 10^3} \approx 33fF \tag{5.3}$$

Because the cut-off frequency of $24MHz$ that is used in this case should not be attenuated, the value of the coupling capacitance is chosen at $100fF$, which is sufficiently higher than the calculated value in equation 5.3.

the last parameter that needs to be calculated is the value of the bias voltage. This value can be calculated using equation 4.4. This equation can be rewritten such that V_{GS} is expressed as a function of g_m. This results in the following equation:

$$V_{GS} = \frac{g_m}{\mu C_{OX}\frac{W}{L}} + V_{TH} \tag{5.4}$$

After substituting the appropriate parameters, the following value for the gate-source voltage V_{GS} is found:

$$V_{GS} = \frac{0.2 \cdot 10^{-3}}{2.75 \cdot 10^{-3}\frac{3.6 \cdot 10^{-6}}{0.36 \cdot 10^{-6}}} + 0.58 \approx 0.6V \tag{5.5}$$

Therefore the bias voltage is set to $0.6V$. Figure 5.3 shows the circuit with the appropriate parameters.

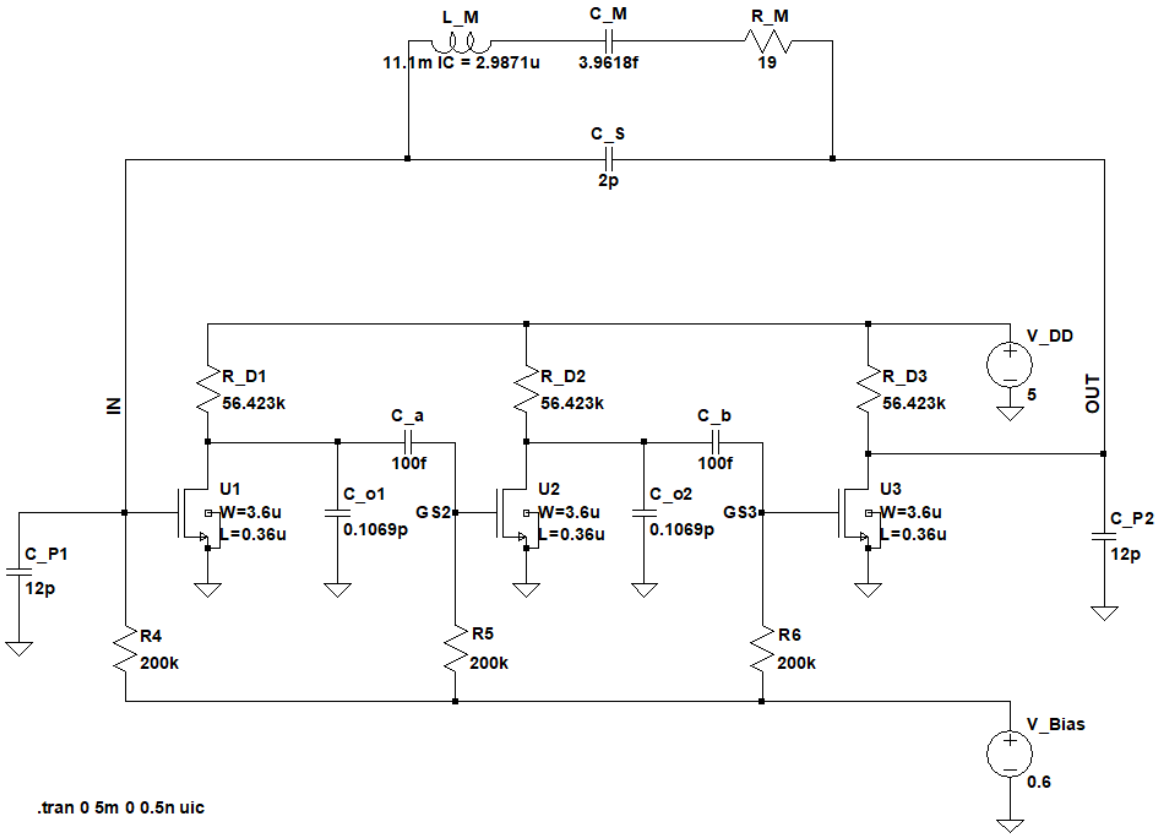

Figure 5.3: Schematic of the circuit for $g_m = 0.2mS$

After running the simulation, the plot of figure 5.4 is obtained, which shows the voltage across the resonator. From this plot it becomes clear that in the beginning the signal has a certain offset. After $t \approx 30\mu s$, this offset has reached its final value. In order to give an explanation of this behaviour, the gate-source voltages of the three inverters are plotted. These plots can be found in figure 5.5. From this figure it becomes clear that after $t \approx 30\mu s$, the gain of the first two inverters increases rapidly, which results in a rapidly increasing gate-source voltage of the third inverter stage.

This increase in gate source voltage also results in an increase in the drain current of the third inverter. However, because for the chosen g_m, the bias is just above the threshold voltage, this increase in current will only appear when the amplitude of the gate-source voltage is positive. When the amplitude becomes negative, the drain current can only decrease by a small amount (because of the low g_m). After this the transistor will be in the sub-threshold region, in which no current will flow. This behavior can also be observed in the plot of figure 5.6. This figure shows a plot of the drain current of the third inverter stage. The peak in drain current that is observed in this plot at a time of approximately $30\mu s$ is caused by the fact that the gate-source voltage of the third inverter stage increases rapidly at this moment in time, as can be seen in figure 5.5. After this point the speed with which the gate source voltage of the third inverter increases becomes less, which causes a decrease in drain current. This can be seen in figure 5.6. Because there is almost no drain current when the amplitude of the gate source voltage gets below the bias voltage, the net amount of drain current of the third inverter stage will increase. This increase in current results in a decrease of the output voltage, which can be observed in figure 5.4. So this is the reason why the voltage across the resonator decreases rapidly until $t \approx 30\mu s$.

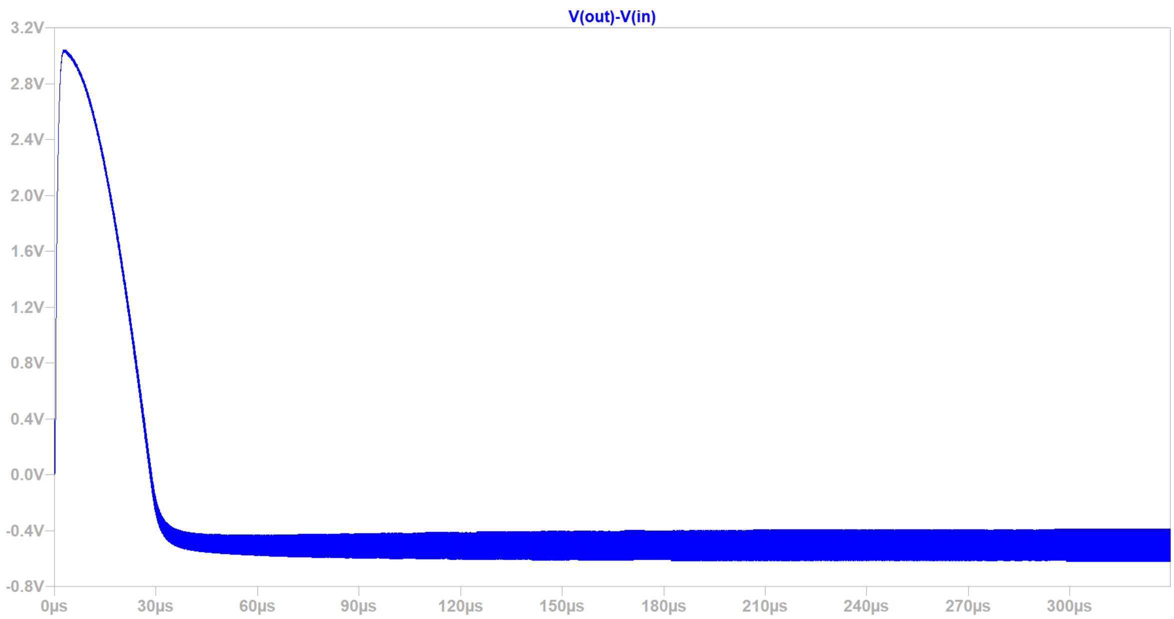

Figure 5.4: Voltage across the resonator for $g_m = 0.2mS$

Because of the decrease in output voltage that is observed in figure 5.4, it is quite difficult to analyse the small signal behavior until $t \approx 30\mu s$. Because of this, the current through the inductor is plotted. This plot will also give information about the growth in amplitude of the signal, while all effects of settling and 'offsets' are removed. The plot of the current through the inductor is shown in figure 5.7. In this plot it is visible that the current increases rapidly until a time of approximately $25\mu s$.

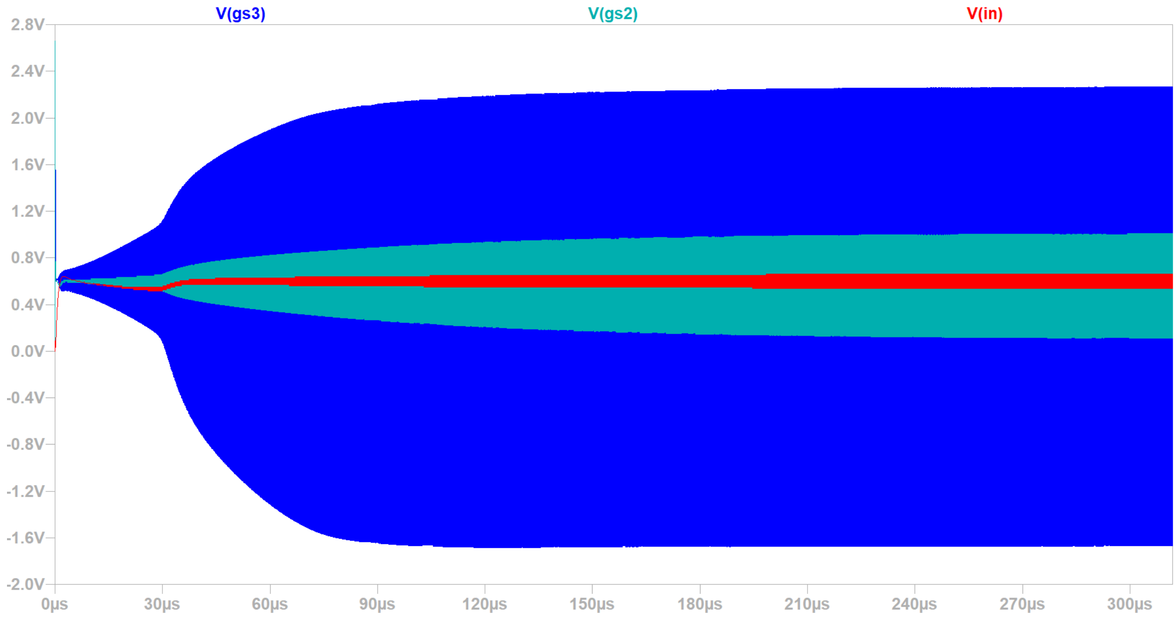

Figure 5.5: Gate-source voltages of the three inverter stages for $g_m = 0.2mS$

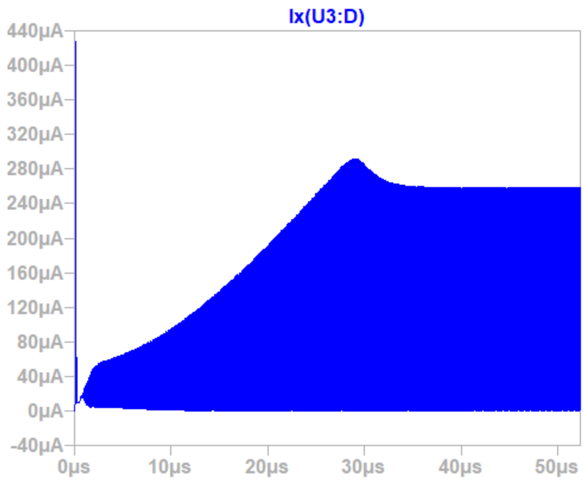

Figure 5.6: Drain current of the third inverter stage for $g_m = 0.2mS$

After this time the speed with which the amplitude grows decreases. In section 5.2 the amplitude growth coefficient will be calculated based on this plot.

As already mentioned earlier, the gate-source voltages of the second and third inverter stage increase rapidly after $t \approx 30\mu s$. This increase can be explained by considering the gate source voltage of the first inverter stage (i.e. V_{in}), which is given in figure 5.5. From this plot it becomes clear that V_{in} has a small increase in offset at $t \approx 30\mu s$. This means that the gate-source voltage of the first inverter stage increases, which results in a bigger drain current. This increase in drain current results in a higher g_m, and therefore the gain increases. This causes the fast amplitude growth of the gate source voltages of the second and third inverter at $t \approx 30\mu s$.

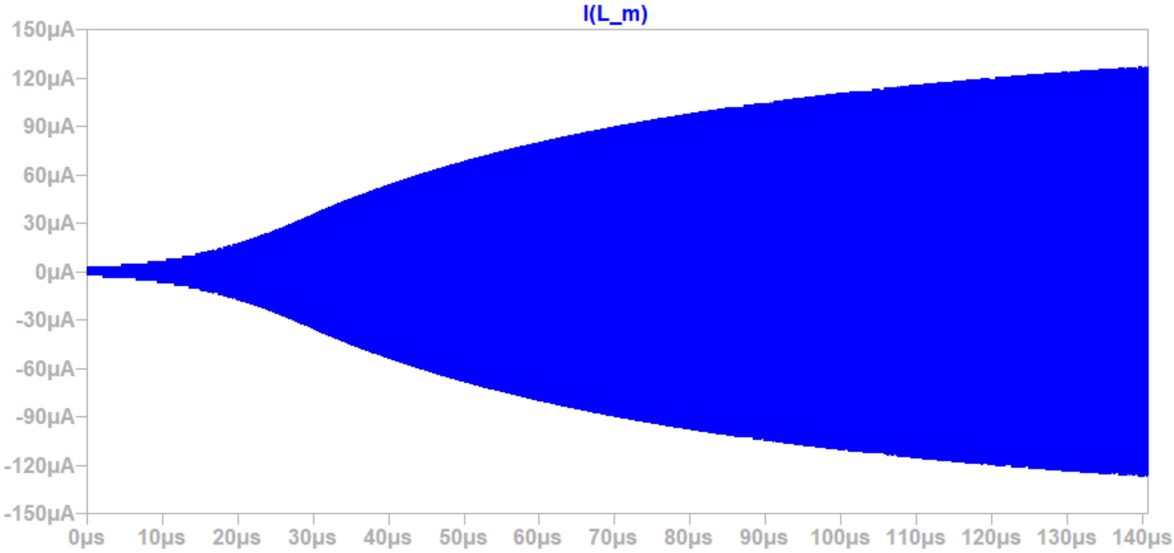

Figure 5.7: Drain current of the third inverter stage for $g_m = 0.2mS$

Another thing that can be noted when looking to figure 5.5 is that it seems like the swing of the voltage amplitude above the bias voltage is smaller than the swing of the voltage amplitude below the bias voltage. This is caused by the fact that the MOSFETs are biased just above the threshold voltage. This limits the voltage swing for voltages below the bias voltage, which increases the net amount of drain current (see figure 5.6). This increase in drain current lowers the voltage that is generated at the output of the MOSFETs, and therefore the bias voltage of the next inverter stage is pulled down.

Furthermore, when looking to figure 5.4 it becomes clear that only a small voltage amplitude can be reached over the resonator, while a much bigger voltage amplitude can be reached after the first and the second inverter stage. This is caused by the fact that the parallel capacitances C_{P1} and C_{P2} have a much higher capacitance than the load capacitances C_{o1} and C_{o2}. Because of this, the drain current of the third MOSFET should be much bigger than the drain current of the first and the second MOSFET in order to generate the same output voltage. Because the g_m of each inverter stage is fixed, the drain current is also fixed. Therefore the amplitude of the output voltage grows much slower than the output voltage of the first and the second inverter stage. When the gate-source voltage of the second inverter has reached its final amplitude, the gain of the last inverter will be equal to one. Therefore the amplitude of the last inverter will also not grow anymore.

5.2 Comparison of simulations with calculations

In this section the simulation results that are obtained in this chapter will be compared to the results of the calculations performed in chapter 4. This will be done by comparing the amplitude growth coefficient and the start-up energy that follow from the simulations with the results obtained during the calculations.

5.2.1 Amplitude growth coefficient

First of all the amplitude growth coefficient will be determined for a g_m of $0.2mS$. This is done by using the plot of figure 5.7. From this plot it can be observed that until $t \approx 25\mu s$ the speed with which the amplitude grows increases, and after this time the increase in amplitude becomes less. In the calculations performed in chapter 4 it is assumed that the amplitude grows exponentially (till $V_{DD}/2$). Because of this, the amplitude growth coefficient should be determined in the region before $t \approx 25\mu s$ in figure 5.7. When this is done, an amplitude growth coefficient of approximately 95000 is obtained. However, during the calculations an amplitude growth coefficient of around 991384 was obtained for a g_m of $0.2mS$, which is about a coefficient ten more. The main reason for this big difference is that the calculations that are performed in chapter 4 are only valid for small signals. Because a low g_m is chosen, the transistors are biased just above the threshold voltage. In this region the transistor behaves highly non-linear, so only small variations in the gate-source voltages of the transistors can already have a big impact on the amplitude growth. This sensitivity for the gate-source voltage also becomes clear when considering the plot of figure 4.12, in which R_{N3} is plotted as a function of g_m. From this figure it becomes clear that only a small change in g_m already has a big influence on R_{N3}, and therefore on the amplitude growth coefficient.

Furthermore the MOSFETS that are used are less accurate for relatively high voltages. Because a supply voltage of $5V$ is used, this could have had an influence on the performance. Besides this, also parasitic effects of the MOSFETs can play a role. The optimum of R_{N3} is only achieved for specific combinations of the inverter resistance R_{inv}, g_m and C_o. Small variations in these parameters caused by for example parasitic effects of the MOSFETs can have a considerable impact on the negative resistance.

5.2.2 Start-up energy

In this section the start-up energy will be derived from the simulations. First of all the start-up energy is determined for a g_m of $0.2mS$. As a measure of the start-up energy, the energy will be determined until a time of $20\mu s$. This is done because for relatively small time values the influence of non-linear effects is small, as can be seen in the plot of 5.7. The start-up energy that is obtained from the simulations is approximately equal to $7,0nJ$. In order to compare this value of the start-up energy with the calculated value of the start-up energy, first the code that is used for calculating the start-up energy should be adjusted. In this code the start-up energy is namely calculated until the amplitude of the voltage across the resonator has reached a value of half the supply voltage. However during the simulation the amplitude is considered at the point where $20\mu s$ have passed. The amplitude at this time appeared to be approximately $43mV$. However, in the calculations the start-up time is considered until the voltage across the resonator has reached a value of $V_{DD}/2$. For a voltage of $43mV$ and a supply voltage V_{DD} of $5V$, this reduction factor should not be equal to 2, but to $5/0.043 \approx 117$. Therefore the time should be considered until the voltage across the resonator has reached a value of $V_{DD}/117$. In order to calculate this new start-up time, equation 3.16 can be rewritten to:

$$t_s = t_{s,tot} - \tau \cdot ln(117) \tag{5.6}$$

With this new start-up time the start-up energy is calculated. The result is a start-up energy of approximately $5.1nJ$. When comparing this value with the simulated value (which was approximately $7,0nJ$), it appears that both values are in the same order of magnitude. As a comparison, the value of the start-up energy until $20\mu s$ will also be calculated and simulated for a g_m of $0.4mS$. For this value of g_m the simulated start-up energy is approximately $8.8nJ$. In order to calculate the start-up energy for this g_m value, again the amplitude of the voltage across the resonator should be known at $t \approx 20\mu s$. This amplitude appeared to be approximately $5.5mV$. The resulting start-up energy that is calculated is approximately given by $4.7nJ$. As becomes clear, this value is smaller than the total start-up energy that was calculated for a g_m of $0.2mS$. This is caused by the fact that the amplitude of this signal at $20\mu s$ is much smaller than the amplitude at $20\mu s$ that was reached for a g_m of $0.2mS$. For $0.4mS$ this was $5.5mV$, while for $0.2mS$ this was $43mV$. This difference in amplitude at $20\mu s$ can be explained when considering the plot of figure 4.12. From this plot it becomes clear that when g_m increases, the negative resistance increases. This increase in negative resistance means that the amplitude growth coefficient decreases, and therefore the amplitude of the voltage across the resonator is much lower for a g_m of $0.4mS$ than for a g_m of $0.2mS$ at a time of $20\mu s$. The fact that this decrease in start-up energy did not appear in the simulations is because the amplitude growth coefficient that was achieved in the simulations was much lower than the amplitude growth coefficient that was calculated. Furthermore, the reason why the simulated start-up energy is higher than the calculated start-up energy for

Table 5.1: Simulation results of amplitude and start-up energy until $t = 20\mu s$, together with the amplitude growth coefficient, for $g_m = 0.2mS$ and $g_m = 0.4mS$

	$g_m = 0.2mS$	$g_m = 0.4mS$
Amplitude at $t = 20\mu s$	$43mV$	$5.5mV$
Start-up energy until $t = 20\mu s$	$7.0nJ$	$8.8nJ$
Amplitude growth coefficient	95000	32579

Table 5.2: Final amplitude for $g_m = 0.2mS$ and $g_m = 0.4mS$ that follows from the simulations, together with the corresponding start-up time and start-up energy

	$g_m = 0.2mS$	$g_m = 0.4mS$	increase factor
Final amplitude	$0.10V$	$0.33V$	3.3
Start-up energy	$60nJ$	$495nJ$	8.3
Start-up time	$96\mu s$	$360\mu s$	6.2

a given value of g_m is because the inverter acts highly nonlinear for the given bias point. A small increase in V_{GS} can cause a big difference in drain current, while the drain current doesn't change a lot when decreasing V_{GS}.

The results that were obtained from the simulations are summarized in table 5.1. From this table it becomes clear that for $g_m = 0.2mS$ a lower start-up energy is achieved than for a g_m of $0.4mS$. This is in correspondence with the conclusions that followed from the calculations in chpater 4. The question that can be asked when looking at table 5.1 is if there is any advantage of increasing the g_m of the three inverter stages. In order to give an answer to this question, the final amplitude across the resonator that is reached for different values of g_m is determined in LTspice. The results are shown in table 5.2. Furthermore, this table also shows the start-up energy that is needed in order to reach this final amplitude, and the corresponding start-up time. From this table it becomes clear the the final amplitude that can be reached for a g_m of $0.4mS$ is bigger than the final amplitude that can be reached for a g_m of $0.2mS$. However, for an increase in amplitude by a factor of 3.3, the start-up energy increases with a factor of approximately 8.3, which is around $8.3/3.3 \approx 2.5$ as high. This increase in start-up energy is however meanly caused by the fact that the start-up time increases when increasing the g_m.

Chapter 6

Conclusions and recommendations

6.1 Conclusions

In this report an analysis is presented in which the optimum design parameters of the three-stage inverter crystal oscillator are determined that result in the minimum start-up energy. From this analysis it followed that when decreasing the value of the transconductance, the total start-up energy decreases rapidly. Furthermore it was found that the negative resistance can theoretically become infinitely big for certain combinations of parameter values. However, it is also demonstrated that when the negative resistance increases, the sensitivity to parameter variations also increases. This can cause the negative resistance to become positive, which means that the crystal oscillator will not operate anymore. Therefore a safety margin can be defined when determining the value of the negative resistance. Furthermore it followed from the analysis that the optimum value of the output capacitances decreases when the transconductance is decreased. Therefore for relatively small values of the transconductance the parasitic capacitances of the transistor have to be taken into account. For which value of the output capacitances these parasitic effects will start to play a significant role depends on the transistors that are used.

Furthermore a comparison is made between the start-up energy of the single stage inverter implementation and the start-up energy of the three-stage inverter implementation. From this comparison it followed that the three-stage inverter implementation has a start-up energy that is several orders of magnitude lower than the start-up energy of the single stage inverter implementation. It also became clear that the minimum start-up energy for the single stage inverter implementation does not occur at the same value of g_m for which the minimum value of R_{N1} is achieved, which was the case for the three-stage inverter implementation.

The results that are obtained from the analysis of the three-stage inverter implementation are tested by performing circuit simulations. From the simulations it followed that the calculated parameters indeed result in a system that oscillates.

However, the final amplitude cannot be reached due to the limited transconductance. Another consequence of the small transconductance is that the MOSFETs are biased just above the threshold voltage, which makes them very sensitive for variations in gate source voltage. The calculations are however based on a certain value for g_m, and therefore on a fixed gate source voltage. These calculations are therefore only valid for small signals. This is the reason why the calculated amplitude growth factor and start-up energy do not exactly match the calculation results. It is however verified with the simulations that a lower g_m results in a lower start-up energy. Furthermore it is shown that a higher amplitude can be reached when increasing the g_m. However, it is also shown that increasing the amplitude with a certain factor increases the start-up energy with a factor that is much higher. Therefore the amplitude of the oscillation should be kept as low as possible in order to minimize the start-up energy.

6.2 Recommendations

During this research the optimum design parameters are found by means of calculations, and the relations were represented in different plots. The results that were obtained from these calculations were used to simulate the oscillator in LTspice. As a next step the circuit can be built in reality, and it can be checked whether the found values indeed result in a properly working oscillator, which has a lower start-up energy than existing oscillators.

In this research it was investigated how the minimum start-up energy of crystal oscillators can be achieved using the three stage inverter implementation. However, during this analysis no requirements where defined about the amplitude of the oscillation that needs to be achieved. The analysis presented in this research can only be used for relatively small values of g_m, because when the value of the transconductance increases, the optimum value of the drain resistance decreases. At a certain point this drain resistance will start to play a significant role in the phase shift generated by the third inverter. In a next research an expression of the negative resistance can be derived which incorporates the effect of this drain resistor.

Bibliography

[1] M.-K. L. R. P. M. Ka-Meng Lei, Pui-In Mak, “A regulation-free sub-0.5v 16/24mhz crystal oscillator for energy-harvesting ble radios with 14.2nj startup energy and 31.8w steady-state power,” ISSCC, February 2018.

[2] J. Murdock and D. Griffith, “Crystal oscillator and crystal selection for the cc26xx and cc13xx family of wireless mcus,” Texas Instruments, December 2015.

[3] E. A. Vittoz, M. G. Degrauwe, and S. Bitz, “High-performance crystal oscillator circuits: Theory and application,” *IEEE JOURNAL OF SOLID-STATE CIRCUITS*, vol. 23, no. 3, pp. 774–783, June 1988.

[4] M. Haque and E. Cox, “Use of the cmos unbuffered inverter in oscillator circuits,” Texas Instruments, January 2004.

[5] A. Rusznyak, “Start-up time of cmos oscillators,” *IEEE transactions on circuits and systems*, vol. cas-34, no. 3, pp. 259–268, March 1987.

[6] B. Razavi, “The crystal oscillator,” IEEE Solid-State Circuits Magazine, Spring 2017.

Appendix A

Mathematical derivations

A.1 Derivation of expression for R_N

For the definition of the different impedances that are used during this derivation, refer to figure 2.3.

$$Z_C = Z_{C_S} // Z_{amp} \tag{A.1}$$

$$Z_{amp} = Re(Z_{amp}) + jIm(Z_{amp}) \tag{A.2}$$

$$Z_C = Z_{C_S} // (Re(Z_{amp}) + jIm(Z_{amp})) \tag{A.3}$$

$$Z_C = \frac{Z_{C_S}(Re(Z_{amp}) + jIm(Z_{amp}))}{Z_{C_S} + Re(Z_{amp}) + jIm(Z_{amp})} \tag{A.4}$$

$$Z_{C_S} = \frac{1}{j\omega_0 C_S} = \frac{1}{j\omega_0 C_S} \cdot \frac{j\omega_0 C_S}{j\omega_0 C_S} = -j\frac{1}{\omega_0 C_S} \tag{A.5}$$

$$Z_C = \frac{-j\frac{1}{\omega_0 C_S}(Re(Z_{amp}) + jIm(Z_{amp}))}{Re(Z_{amp}) + j(-\frac{1}{\omega_0 C_S} + Im(Z_{amp}))} \cdot \frac{Re(Z_{amp}) - j(-\frac{1}{\omega_0 C_S} + Im(Z_{amp}))}{Re(Z_{amp}) - j(-\frac{1}{\omega_0 C_S} + Im(Z_{amp}))} \tag{A.6}$$

$$Z_C = \frac{-j\frac{1}{\omega_0 C_S}Re(Z_{amp}) + jIm(Z_{amp}))(Re(Z_{amp}) + j(\frac{1}{\omega_0 C_S} - Im(Z_{amp}))}{(Re(Z_{amp}))^2 + (-\frac{1}{\omega_0 C_S + Im(Z_{amp}))^2}} \tag{A.7}$$

$$Re(Z_C) = \frac{\frac{1}{\omega_0 C_S}Im(Z_{amp})Re(Z_{amp}) + (\frac{1}{\omega_0 C_S})^2 Re(Z_{amp}) - \frac{1}{\omega_0 C_S}Re(Z_{amp})Im(Z_{amp})}{(Re(Z_{amp}))^2 + (-\frac{1}{\omega_0 C_S} + Im(Z_{amp}))^2} \tag{A.8}$$

$$Re(Z_C) = \frac{\frac{1}{\omega_0^2 C_S^2} Re(Z_{amp})}{(Re(Z_{amp}))^2 + \frac{1}{\omega_0^2 C_S^2} - 2\frac{1}{\omega_0 C_S} Im(Z_{amp} + (Im(Z_{amp}))^2} \tag{A.9}$$

$$Re(Z_C) = \frac{Re(Z_{amp})}{(\omega_0 C_S Re(Z_{amp}))^2 + 1 - 2\omega_0 C_S Im(Z_{amp}) + (\omega_0 C_S Im(Z_{amp}))^2} \tag{A.10}$$

$$Re(Z_C) = \frac{Re(Z_{amp})}{(\omega_0 C_S Re(Z_{amp}))^2 + (1 - \omega_0 C_S Im(Z_{amp}))^2} \tag{A.11}$$

$$R_N = -Re(Z_{amp}) \tag{A.12}$$

$$R_N = -\frac{Re(Z_{amp})}{(\omega_0 C_S Re(Z_{amp}))^2 + (1 - \omega_0 C_S Im(Z_{amp}))^2} \tag{A.13}$$

A.2 Derivation of expression for Z_{amp-3}

In order to calculate the impedance Z_{amp-3}, a voltage V_S will be applied to this impedance, which generates a current I_S. The impedance Z_{amp-3} is then defined as:

$$Z_{amp-3} = \frac{V_S}{I_S} \tag{A.14}$$

In figure A.1 all the parameters are defined that are needed to calculate the impedance Z_{amp-3}. First a general relation between V_S and I_S is derived:

$$V_S = V_{out} - V_{in} \tag{A.15}$$

$$V_S = \frac{1}{j\omega_0 2C_L} I_2 - \frac{1}{j\omega_0 2C_L} I_1 \tag{A.16}$$

$$V_S = \frac{1}{j\omega_0 2C_L}(I_2 - I_1) \tag{A.17}$$

An expression for the current I_2 can be derived as follows:

$$I_2 = I_S + I_{inv_3} \tag{A.18}$$

$$I_2 = I_S + g_{m3} V_{o2} \tag{A.19}$$

$$I_2 = I_S + g_{m3} I_{inv2} Z_{o2} \tag{A.20}$$

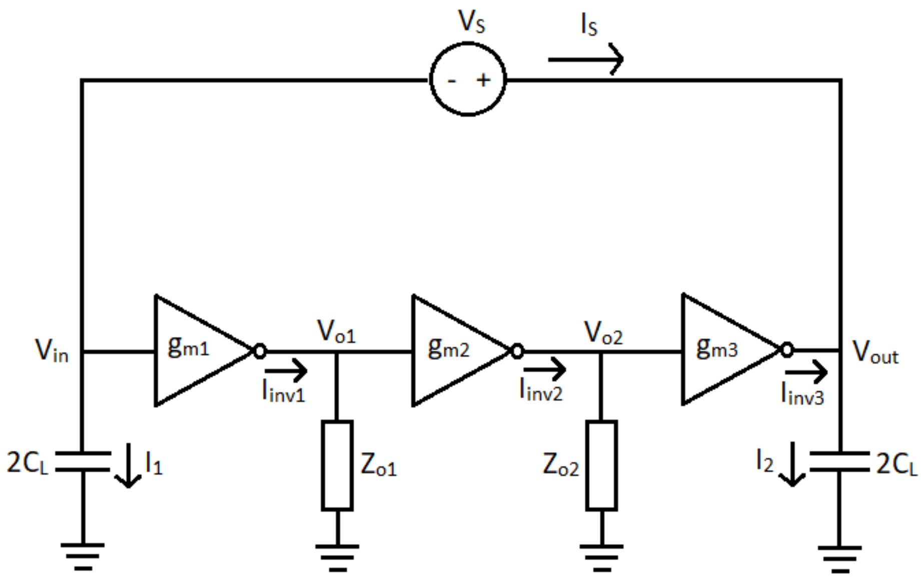

Figure A.1: Definition of the different parameters in order to calculate Z_{amp-3}

$$I_2 = I_S + g_{m3}g_{m2}V_{o1}Z_{o2} \tag{A.21}$$

$$I_2 = I_S + g_{m3}g_{m2}I_{inv1}Z_{o1}Z_{o2} \tag{A.22}$$

$$I_2 = I_S + g_{m3}g_{m2}g_{m1}V_{in}Z_{o1}Z_{o2} \tag{A.23}$$

V_{in} is the voltage over the left capacitor in figure A.1, therefore the voltage V_{in} is defined as:

$$V_{in} = \frac{1}{j\omega_0 2C_L} \cdot -I_1 \tag{A.24}$$

$$I_1 = -I_S \tag{A.25}$$

$$V_{in} = \frac{1}{j\omega_0 2C_L} I_S \tag{A.26}$$

Substituting equation A.26 in equation A.28 gives:

$$I_2 = I_S + g_{m1}g_{m2}g_{m3}Z_{o1}Z_{o2}\frac{1}{j\omega_0 2C_L} I_S \tag{A.27}$$

$$I_2 = (1 + g_{m1}g_{m2}g_{m3}Z_{o1}Z_{o2}\frac{1}{j\omega_0 2C_L}) I_S \tag{A.28}$$

Next equation A.25 and A.28 can be substituted in equation A.17, which results in:

$$V_S = \frac{1}{j\omega_0 2C_L}((1 + g_{m1}g_{m2}g_{m3}Z_{o1}Z_{o2}\frac{1}{j\omega_0 2C_L})I_S + I_S) \tag{A.29}$$

$$V_S = \frac{1}{j\omega_0 2C_L}(1 + g_{m1}g_{m2}g_{m3}Z_{o1}Z_{o2}\frac{1}{j\omega_0 2C_L} + 1)I_S \tag{A.30}$$

$$Z_{amp-3} = \frac{V_S}{I_S} = \frac{1}{j\omega_0 2C_L}(g_{m1}g_{m2}g_{m3}Z_{o1}Z_{o2}\frac{1}{j\omega_0 2C_L} + 2) \tag{A.31}$$

$$Z_{amp-3} = \frac{g_{m1}g_{m2}g_{m3}Z_{o1}Z_{o2}\frac{1}{j\omega_0 2C_L}}{j\omega_0 2C_L} + \frac{1}{j\omega_0 C_L} \tag{A.32}$$

The impedances Z_{o1} and Z_{o2} consist of the capacitances C_{o1} and C_{o2} in parallel with the output resistances of the transistors r_{o1} and r_{o2}. This means that:

$$Z_{o1} = Z_{C_{o1}}//Z_{r_{o1}} = \frac{\frac{1}{j\omega_0 C_{o1}}r_{o1}}{\frac{1}{j\omega_0 C_{o1}} + r_{o1}} = \frac{r_{o1}}{1 + j\omega_0 C_{o1}r_{o1}} \tag{A.33}$$

$$Z_{o2} = Z_{C_{o2}}//Z_{r_{o2}} = \frac{\frac{1}{j\omega_0 C_{o2}}r_{o2}}{\frac{1}{j\omega_0 C_{o2}} + r_{o2}} = \frac{r_{o2}}{1 + j\omega_0 C_{o2}r_{o2}} \tag{A.34}$$

Substituting equation A.33 and A.34 in equation A.32 gives:

$$Z_{amp-3} = \frac{g_{m1}g_{m2}g_{m3}\frac{r_{o1}}{1+j\omega_0 C_{o1}r_{o1}}\frac{r_{o2}}{1+j\omega_0 C_{o2}r_{o2}}\frac{1}{j\omega_0 2C_L}}{j\omega_0 2C_L} + \frac{1}{j\omega_0 C_L} \tag{A.35}$$

$$Z_{amp-3} = -\frac{g_{m1}g_{m2}g_{m3}r_{o1}r_{o2}}{4\omega_0^2 C_L^2(1 + j\omega_0 C_{o1}r_{o1})(1 + j\omega_0 C_{o2}r_{o2})} + \frac{1}{j\omega_0 C_L} \tag{A.36}$$

In order to reduce the amount of calculations, the following variables will be defined:

$$a = g_{m1}r_{o1}g_{m2}r_{o2}g_{m3} \tag{A.37}$$

$$b = \omega_0 C_{o1}r_{o1} \tag{A.38}$$

$$c = \omega_0 C_{o2}r_{o2} \tag{A.39}$$

$$d = \omega_0 C_L \tag{A.40}$$

Equation A.36 can now be written as:

$$Z_{amp-3} = -\frac{a}{4d^2(1 + jb)(1 + jc)} + \frac{1}{jd} \tag{A.41}$$

The expression given in equation A.41 can be rewritten in a real part and an imaginary part. First the real and imaginary part of the denominator of the first term of equation A.36 will be determined:

$$4d^2(1+jb)(1+jc) = \tag{A.42}$$

$$(4d^2 + j4bd^2)(1+jc) = \tag{A.43}$$

$$4d^2 + j4cd^2 + j4bd^2 - 4bcd^2 = \tag{A.44}$$

$$4d^2(1-bc) + j4d^2(b+c) \tag{A.45}$$

Using equation A.45, the first term of equation A.41 can now be written as:

$$-\frac{a}{4d^2(1+jb)(1+jc)} = \tag{A.46}$$

$$-\frac{a}{4d^2(1-bc) + j4d^2(b+c)} = \tag{A.47}$$

$$-\frac{a}{4d^2(1-bc) + j4d^2(b+c)} \cdot \frac{4d^2(1-bc) - j4d^2(b+c)}{4d^2(1-bc) - j4d^2(b+c)} = \tag{A.48}$$

$$-\frac{4ad^2(1-bc) - j4ad^2(b+c)}{16d^4(1-bc)^2 + 16d^4(b+c)^2} = \tag{A.49}$$

$$-\frac{a(1-bc) - ja(b+c)}{4d^2(1-bc)^2 + 4d^2(b+c)^2} = \tag{A.50}$$

$$-\frac{a(1-bc) - ja(b+c)}{4d^2((1-bc)^2 + (b+c)^2)} = \tag{A.51}$$

$$-\frac{a(1-bc) - ja(b+c)}{4d^2(1 - 2bc + b^2c^2 + b^2 + 2bc + c^2)} = \tag{A.52}$$

$$-\frac{a(1-bc) - ja(b+c)}{4d^2(1 + b^2 + c^2 + b^2c^2)} = \tag{A.53}$$

$$-\frac{a(1-bc) - ja(b+c)}{4d^2(1+b)^2(1+c)^2} = \tag{A.54}$$

$$-\frac{a(1-bc)}{4d^2(1+b)^2(1+c)^2} + j\frac{a(b+c)}{4d^2(1+b)^2(1+c)^2} \tag{A.55}$$

Also the second term of equation A.41 has to be split in a real part and an imaginary part:

$$\frac{1}{jd} = \frac{1}{jd} \cdot \frac{jd}{jd} = -j\frac{1}{d} \tag{A.56}$$

Substituting equation A.55 and A.56 back in equation A.41 gives:

$$Z_{amp-3} = -\frac{a(1-bc)}{4d^2(1+b)^2(1+c)^2} + j\frac{a(b+c)}{4d^2(1+b)^2(1+c)^2} - j\frac{1}{d} \tag{A.57}$$

$$Z_{amp-3} = -\frac{a(1-bc)}{4d^2(1+b)^2(1+c)^2} + j(\frac{a(b+c)}{4d^2(1+b)^2(1+c)^2} - \frac{1}{d}) \tag{A.58}$$

Inserting the expressions for a, b, c and d in equation A.58 gives:

$$\begin{aligned} Z_{amp-3} = &-\frac{g_{m1}r_{o1}g_{m2}r_{o2}g_{m3}(1-\omega_0^2 r_{o1}C_{o1}r_{o2}C_{o2})}{4\omega_0^2 C_L^2(1+(\omega_0 r_{o1}C_{o1})^2)(1+(\omega_0 r_{o2}C_{o2})^2)} + \\ &j(\frac{g_{m1}r_{o1}g_{m2}r_{o2}g_{m3}\omega_0(r_{o1}C_{o1}+r_{o2}C_{o2})}{4\omega_0 C_L^2(1+(\omega_0 r_{o1}C_{o1})^2)(1+(\omega_0 r_{o2}C_{o2})^2)} - \frac{1}{\omega_0 C_L}) \end{aligned} \tag{A.59}$$

$$\begin{aligned} Z_{amp-3} = &-\frac{g_{m1}r_{o1}g_{m2}r_{o2}g_{m3}(1-\omega_0^2 r_{o1}C_{o1}r_{o2}C_{o2})}{4\omega_0^2 C_L^2(1+(\omega_0 r_{o1}C_{o1})^2)(1+(\omega_0 r_{o2}C_{o2})^2)} + \\ &j\frac{1}{\omega_0 C_L}(\frac{g_{m1}r_{o1}g_{m2}r_{o2}g_{m3}(r_{o1}C_{o1}+r_{o2}C_{o2})}{4C_L(1+(\omega_0 r_{o1}C_{o1})^2)(1+(\omega_0 r_{o2}C_{o2})^2)} - 1) \end{aligned} \tag{A.60}$$